

Absence of Elovl6 attenuates steatohepatitis but promotes gallstone formation in a lithogenic diet-fed Ldlr^{-/-} mouse model

著者	久芳 素子
year	2016
その他のタイトル	Elovl6欠損は胆石形成食負荷LDL受容体欠損マウスにおいて脂肪性肝炎を抑制するが、胆石形成を促進する
学位授与大学	筑波大学 (University of Tsukuba)
学位授与年度	2015
報告番号	12102甲第7850号
URL	http://hdl.handle.net/2241/00143978

筑波大学

博士（医学）学位論文

**Absence of *Elovl6* attenuates steatohepatitis but
promotes gallstone formation in a lithogenic diet-fed
Ldlr^{-/-} mouse model**


(*Elovl6* 欠損は胆石形成食負荷 LDL 受容体欠損マウスに
おいて脂肪性肝炎を抑制するが、胆石形成を促進する)

2 0 1 5

筑波大学大学院博士課程人間総合科学研究科

久 芳 素 子

SCIENTIFIC REPORTS



OPEN

Absence of *Elovl6* attenuates steatohepatitis but promotes gallstone formation in a lithogenic diet-fed *Ldlr*^{-/-} mouse model

Received: 04 August 2015

Accepted: 30 October 2015

Published: 01 December 2015

Motoko Kuba¹, Takashi Matsuzaka¹, Rie Matsumori¹, Ryo Saito¹, Naoko Kaga³, Hikari Taka³, Kei Ikehata⁴, Naduki Okada¹, Takuya Kikuchi¹, Hiroshi Ohno¹, Song-lee Han¹, Yoshinori Takeuchi¹, Kazuto Kobayashi¹, Hitoshi Iwasaki¹, Shigeru Yatoh¹, Hiroaki Suzuki¹, Hirohito Sone⁵, Naoya Yahagi¹, Yoji Arakawa⁴, Tsutomu Fujimura³, Yoshimi Nakagawa^{1,2}, Nobuhiro Yamada¹ & Hitoshi Shimano^{1,2}

Nonalcoholic steatohepatitis (NASH) is a progressive form of nonalcoholic fatty liver disease (NAFLD) that can develop into liver cirrhosis and cancer. Elongation of very long chain fatty acids (ELOVL) family member 6 (*Elovl6*) is a microsomal enzyme that regulates the elongation of C12–16 saturated and monounsaturated fatty acids (FAs). We have previously shown that *Elovl6* plays an important role in the development of hepatic insulin resistance and NASH by modifying FA composition. Recent studies have linked altered hepatic cholesterol homeostasis and cholesterol accumulation to the pathogenesis of NASH. In the present study, we further investigated the role of *Elovl6* in the progression of lithogenic diet (LD)-induced steatohepatitis. We showed that the absence of *Elovl6* suppresses hepatic lipid accumulation, plasma total cholesterol and total bile acid (BA) levels in LDL receptor-deficient (*Ldlr*^{-/-}) mice challenged with a LD. The absence of *Elovl6* also decreases hepatic inflammation, oxidative stress and liver injury, but increases the formation of cholesterol crystals in the less dilated gallbladder. These findings suggest that *Elovl6*-mediated changes in hepatic FA composition, especially oleic acid (C18:1n-9), control handling of hepatic cholesterol and BA, which protects against hepatotoxicity and steatohepatitis, but promotes gallstone formation in LD-fed *Ldlr*^{-/-} mice.

Currently, nonalcoholic fatty liver disease (NAFLD) is the most common form of chronic liver disease worldwide^{1–4}. NAFLD encompasses a wide spectrum of conditions associated with the over-accumulation of lipids in the liver, ranging from steatosis to nonalcoholic steatohepatitis (NASH), which includes hepatitis and fibrosis. The mechanisms of disease progression in NASH are not yet completely understood.

It has been hypothesized that the development of NASH requires ‘two hits’⁵. The first hit is the development of hepatic steatosis and the second hit includes cellular stresses such as oxidative stress and elevated levels of proinflammatory cytokines. Recently, growing evidence suggests that simple steatosis

¹Department of Internal Medicine (Endocrinology and Metabolism), Faculty of Medicine, University of Tsukuba, 1-1-1 Tennodai, Tsukuba, Ibaraki 305-8575, Japan. ²International Institute for Integrative Sleep Medicine (WPI-IIMS), University of Tsukuba, Tsukuba, Ibaraki, Japan. ³Laboratory of Proteomics and Biomolecular Science, Biomedical Research Center, Juntendo University Graduate School of Medicine, Tokyo 113-8421, Japan. ⁴Faculty of Life and Environmental Sciences, University of Tsukuba, 1-1-1 Tennodai, Tsukuba, Ibaraki 305-8572, Japan. ⁵Department of Internal Medicine, Faculty of Medicine, Niigata University, 1-754 Asahimachi, Niigata 951-8510, Japan. Correspondence and requests for materials should be addressed to T.M. (email: t-matsuz@md.tsukuba.ac.jp) or H.S. (email: hshimano@md.tsukuba.ac.jp)

and NASH may be two separate diseases. In this ‘multiple parallel hit’ hypothesis, the accumulated lipotoxic/proinflammatory lipid species interact with proinflammatory factors to cause progression to NASH; whereas, in other cases the liver develops steatosis and remains free of inflammation^{6,7}. Therefore, it is important to identify toxic lipids. Although large epidemiological studies have suggested that triglyceride (TG)-mediated pathways may negatively affect NAFLD⁸, recent evidence indicates that TGs may, in fact, have a protective function^{9,10}. Several studies have shown that the dysregulation of cholesterol metabolism is involved in the pathogenesis of NAFLD. Epidemiological data indicate a relationship between increased cholesterol intake and the risk and severity of NAFLD^{11,12}. In addition, experimental models have demonstrated that free cholesterol loading precipitates steatohepatitis¹³.

The fatty acid (FA) composition of lipid species could be another determinant of the development of liver injury. Elongation of very long fatty acids (ELOVL) family member 6 (Elovl6) is a microsomal enzyme that regulates the elongation of C12–16 saturated and monounsaturated FAs^{14,15}. The absence of Elovl6 function reduces stearate (C18:0) and oleate (C18:1n-9) levels and increases palmitate (C16:0) and palmitoleate (C16:1n-7) levels¹⁶. In our previous study, we reported that mice with a targeted disruption of Elovl6 (*Elovl6*^{-/-}) were protected against the development of hepatic insulin resistance¹⁶, the deterioration of the insulin secretory function of pancreatic β -cells¹⁷ and macrophage foam cell formation¹⁸. Our findings suggest that the alteration of FA composition by Elovl6 deficiency not only affects lipid accumulation but also plays a vital role in a wide range of cellular functions and in disease progression.

Low density lipoprotein (LDL) receptor (LDLR)-deficient (*Ldlr*^{-/-}) mice have been used in numerous studies as a model for atherosclerosis. It has been reported that *Ldlr*^{-/-} mice fed a high-cholesterol diet have increased sensitivity to inflammation, apoptosis and fibrosis of the liver^{19–21}. In addition, *Ldlr*^{-/-} mice have a human-like lipoprotein profile²². Therefore, *Ldlr*^{-/-} mice can be used to study the early progression of NASH. We recently reported that atherogenic high-fat (AHF) diet-induced hepatic inflammation, oxidative damage and fibrosis in the liver were attenuated in *Elovl6*^{-/-} mice, despite comparable hepatosteatosis in *Elovl6*^{-/-} mice and wild-type mice²³. To advance our understanding of the progression of NASH and to investigate the impact of Elovl6 deficiency on the development and progression of NASH, in the present study we used a lithogenic diet (LD) to induce NASH in *Ldlr*^{-/-} mice.

Results

Effects of Elovl6 deficiency on body and tissue weight alterations in LD-fed *Ldlr*^{-/-} mice. Elovl6 and LDLR deficient mice were crossed to generate mice with deficiencies of both Elovl6 (*Elovl6*^{-/-}) and LDLR (*Ldlr*^{-/-}). Mice aged 11–16 weeks were fed a standard diet (SD) or an LD for 4 weeks. On an SD, *Elovl6*^{-/-}*Ldlr*^{-/-} mice had similar body weight to the *Elovl6*^{+/+}*Ldlr*^{-/-} mice (Fig. 1A). The LD showed a trend to decrease body weight in *Elovl6*^{+/+}*Ldlr*^{-/-} mice and to increase body weight in *Elovl6*^{-/-}*Ldlr*^{-/-} mice. As a result, LD-fed *Elovl6*^{+/+}*Ldlr*^{-/-} mice were significantly lighter than LD-fed *Elovl6*^{-/-}*Ldlr*^{-/-} mice. Daily food intake in LD-fed *Elovl6*^{-/-}*Ldlr*^{-/-} mice was not significantly different compared with LD-fed *Elovl6*^{+/+}*Ldlr*^{-/-} mice. The LD for 4 weeks increased liver weights in both *Elovl6*^{+/+}*Ldlr*^{-/-} and *Elovl6*^{-/-}*Ldlr*^{-/-} mice compared with their SD-fed counterparts, but *Elovl6*^{-/-}*Ldlr*^{-/-} mice showed less LD-induced liver weight gain compared with *Elovl6*^{+/+}*Ldlr*^{-/-} mice (Fig. 1B). It is well known that an LD increases the amount of bile, leads to supersaturation of the bile with cholesterol and increases susceptibility to gallstone formation. Supporting this, gallbladder weights were markedly increased in LD-fed *Elovl6*^{+/+}*Ldlr*^{-/-} mice (Fig. 1C). Conversely, absence of Elovl6 abolished LD-induced gallbladder enlargement, indicating a decrease in the amount of bile in *Elovl6*^{-/-}*Ldlr*^{-/-} mice. LD-fed *Elovl6*^{+/+}*Ldlr*^{-/-} mice exhibited significant reductions in epididymal white adipose tissue (WAT) weight compared with SD-fed *Elovl6*^{+/+}*Ldlr*^{-/-} mice (Fig. 1D). In contrast, there was no significant difference in WAT weight between LD-fed and SD-fed *Elovl6*^{-/-}*Ldlr*^{-/-} mice.

Elovl6 deficiency reduces plasma total cholesterol and bile acid levels in LD-fed *Ldlr*^{-/-} mice. In mice fed an SD, plasma levels of total cholesterol (TC), TG, free fatty acid (FFA) and total bile acid (TBA) were not significantly different between *Elovl6*^{+/+}*Ldlr*^{-/-} and *Elovl6*^{-/-}*Ldlr*^{-/-} mice (Fig. 2A–D). After 4 weeks on an LD, plasma TC, TG and TBA levels in *Elovl6*^{+/+}*Ldlr*^{-/-} mice were markedly elevated compared with levels in SD-fed *Elovl6*^{+/+}*Ldlr*^{-/-} mice as a consequence of dietary loading of cholesterol, fat and cholic acid (CA) in the LD. However, *Elovl6*^{-/-}*Ldlr*^{-/-} mice were strongly resistant to these changes caused by the LD. Compared with LD-fed *Elovl6*^{+/+}*Ldlr*^{-/-} mice, LD-fed *Elovl6*^{-/-}*Ldlr*^{-/-} mice had significantly lower plasma TC, and plasma TBA levels were markedly suppressed (Fig. 2A, D). High-performance liquid chromatography (HPLC) revealed that very low density lipoprotein (VLDL) and LDL cholesterol, the major cholesterol fraction in *Ldlr*^{-/-} mice on an LD, was reduced and HDL cholesterol was increased in LD-fed *Elovl6*^{-/-}*Ldlr*^{-/-} mice compared with LD-fed *Elovl6*^{+/+}*Ldlr*^{-/-} mice (Fig. 2E).

Elovl6 deficiency suppresses hepatic lipid accumulation but promotes cholesterol crystallization and gallstone formation in *Ldlr*^{-/-} mice. Photographs of the opened abdominal cavities of both groups on the LD show that the livers of LD-fed *Elovl6*^{+/+}*Ldlr*^{-/-} mice were pale, but the livers of LD-fed *Elovl6*^{-/-}*Ldlr*^{-/-} mice were red (Fig. 3A). However, in contrast to *Elovl6*^{+/+}*Ldlr*^{-/-} mice after 4 weeks of the LD, the LD-fed *Elovl6*^{-/-}*Ldlr*^{-/-} mice had opaque gallbladders and increased numbers of aggregated cholesterol gallstones in greenish bile. The incidence of gallstones was higher in

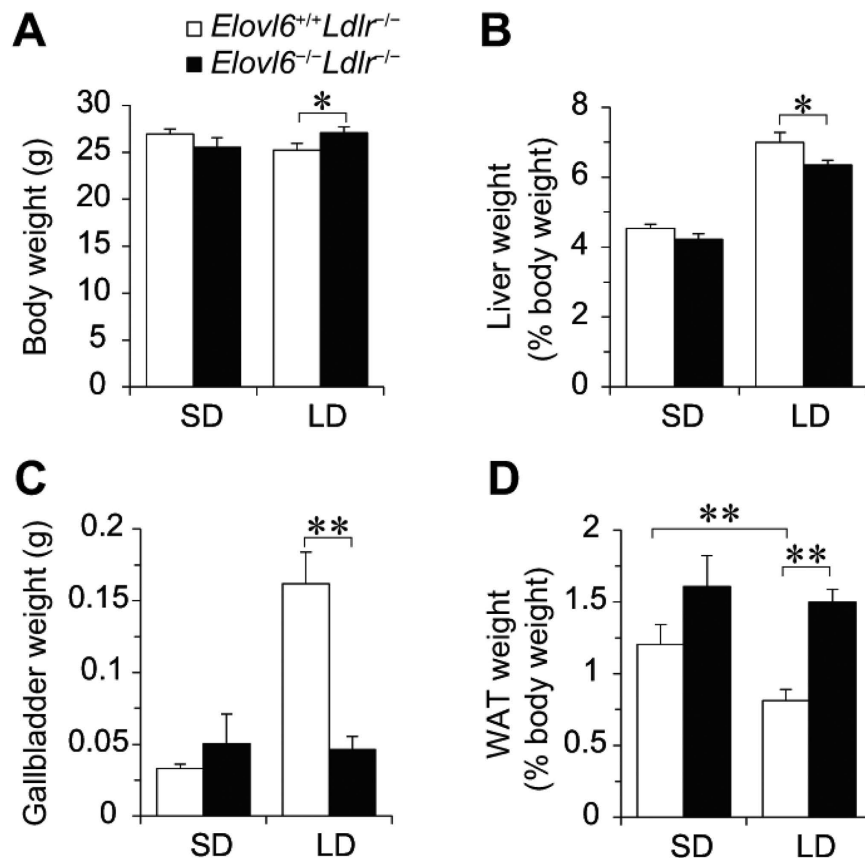


Figure 1. Total body, liver, white adipose tissue (WAT) and gallbladder weights of *Ldlr*^{-/-} mice lacking *Elov6*. (A) Whole body, (B) liver, (C) gallbladder and (D) perigonadal WAT weights were measured in *Elov6*^{+/+}*Ldlr*^{-/-} and *Elov6*^{-/-}*Ldlr*^{-/-} mice fed a standard diet (SD) or a lithogenic diet (LD) for 4 weeks (n = 8–13 per group, *P < 0.05, **P < 0.01).

Elov6^{-/-}*Ldlr*^{-/-} mice (80%) than in *Elov6*^{+/+}*Ldlr*^{-/-} mice (37.5%) after 4-week feeding of LD (Fig. 3B). Microscopic examination of the gallbladder bile from LD-fed *Elov6*^{-/-}*Ldlr*^{-/-} mice revealed numerous large cholesterol monohydrate crystals; whereas, bile from LD-fed *Elov6*^{+/+}*Ldlr*^{-/-} mice was largely free of cholesterol precipitates, with only occasional aggregated vesicles in most animals (Fig. 3C). The LD markedly increased liver TC and increased liver TG levels in *Elov6*^{+/+}*Ldlr*^{-/-} mice. In LD-fed *Elov6*^{-/-}*Ldlr*^{-/-} mice, the liver TC increase was reduced to half that observed in *Elov6*^{+/+}*Ldlr*^{-/-} mice and there was no increase in TG levels (Fig. 3D, E). The LD increased liver TBA levels in both genotypes, but unlike plasma levels, there was no significant difference between the groups (Fig. 3F). Bile TC, TBA, phospholipid (PL), faecal TC and TBA levels were similar between LD-fed *Elov6*^{+/+}*Ldlr*^{-/-} and LD-fed *Elov6*^{-/-}*Ldlr*^{-/-} mice (see Supplementary Fig. S1 online). These results suggest that it was the change in hepatic lipid metabolism in LD-fed *Elov6*^{-/-}*Ldlr*^{-/-} mice that suppressed hepatic cholesterol and triglycerides accumulation and enhanced gallstone formation, rather than a functional change in the gallbladder or intestine.

Histological examination of the livers revealed some inflammatory cell infiltration in SD-fed *Elov6*^{+/+}*Ldlr*^{-/-} mice, but not in SD-fed *Elov6*^{-/-}*Ldlr*^{-/-} mice (Fig. 4A). Inflammatory cell infiltration was exacerbated in LD-fed *Elov6*^{+/+}*Ldlr*^{-/-} mice, but markedly ameliorated in LD-fed *Elov6*^{-/-}*Ldlr*^{-/-} mice. The protection from inflammation and liver damage associated with *Elov6* deficiency was reflected in a significantly lower hepatic lobular inflammatory grade (evaluated by the number of inflammatory foci in hematoxylin & eosin [H&E]-stained liver sections) and plasma alanine aminotransferase (ALT) levels in LD-fed *Elov6*^{-/-}*Ldlr*^{-/-} mice compared with LD-fed *Elov6*^{+/+}*Ldlr*^{-/-} mice (Fig. 4B,C).

***Elov6* deficiency leads to decreased hepatic C18:1 in LD-fed *Ldlr*^{-/-} mice.** FA composition analysis identified that lack of *Elov6* modified the FA profiles of total lipid, cholesterol ester (CE), TG and PL fractions in the livers of *Ldlr*^{-/-} mice fed an SD or an LD (Fig. 5). Compared with SD-fed *Elov6*^{+/+}*Ldlr*^{-/-} mice, the total lipid fractions of SD-fed *Elov6*^{-/-}*Ldlr*^{-/-} mice had increased C16:0 and C18:2n-6 and decreased C20:3n-6, C22:0 and C24:0 (Fig. 5A). Compared with LD-fed *Elov6*^{+/+}*Ldlr*^{-/-} mice, the total lipid fractions of LD-fed *Elov6*^{-/-}*Ldlr*^{-/-} mice had increased C16:0 and a tendency toward decreased C18:1n-9. In the CE fraction, compared with LD-fed *Elov6*^{+/+}*Ldlr*^{-/-} mice, the livers

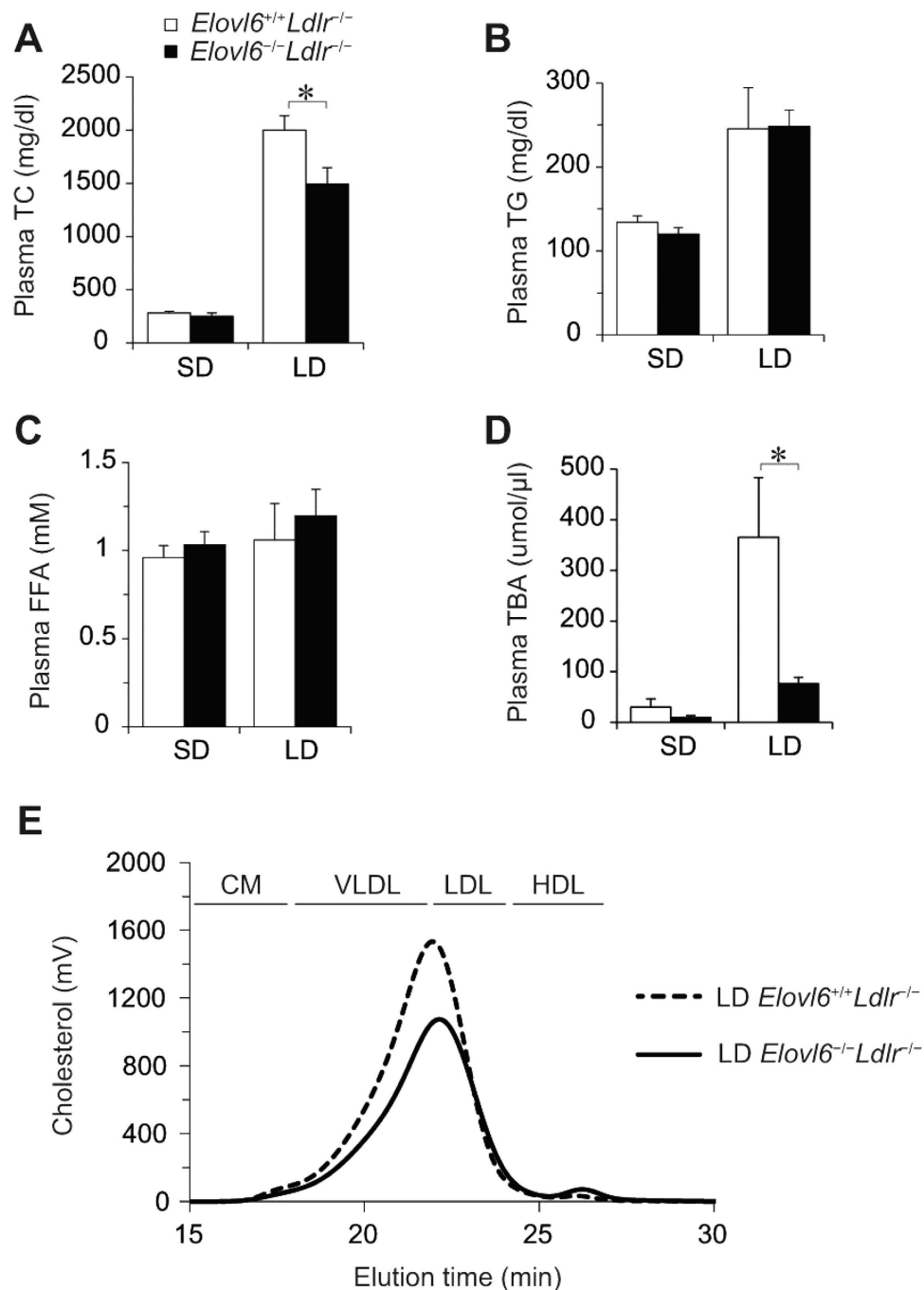


Figure 2. Plasma lipid and lipoprotein profiles of lithogenic diet (LD)-fed *Ldlr*^{-/-} mice lacking *Elovl6*. (A) Plasma total cholesterol (TC), (B) triglyceride (TG), (C) free fatty acid (FFA) and (D) total bile acid (TBA) levels in *Elovl6*^{+/+}*Ldlr*^{-/-} and *Elovl6*^{-/-}*Ldlr*^{-/-} mice fed a standard diet (SD) or an LD for 4 weeks (n = 8–13 per group). (E) High performance liquid chromatography lipoprotein profiles of pooled plasma samples from *Elovl6*^{+/+}*Ldlr*^{-/-} and *Elovl6*^{-/-}*Ldlr*^{-/-} mice fed an LD for 4 weeks (n = 3–4 per group). Peaks for very low density lipoprotein (VLDL), low density lipoprotein (LDL) and high density lipoprotein (HDL) are indicated. **P* < 0.05, ***P* < 0.01.

of the LD-fed *Elovl6*^{-/-}*Ldlr*^{-/-} mice had a decreased relative amount of C18:1n-9, whereas the relative amount of C16:0 was increased (Fig. 5B). In the TG fraction, the only significant difference between the groups was increased C16:0 in the livers of SD-fed *Elovl6*^{-/-}*Ldlr*^{-/-} mice compared with SD-fed *Elovl6*^{+/+}*Ldlr*^{-/-} mice (Fig. 5C). In the PL fraction, the relative amounts of C16:0 and C16:1n-7 were increased in the livers of SD-fed *Elovl6*^{-/-}*Ldlr*^{-/-} mice compared with SD-fed *Elovl6*^{+/+}*Ldlr*^{-/-} mice (Fig. 5D). In the PL fraction in LD-fed mice, the relative amounts of C12:0, C14:0, C16:0, C16:1n-7, and C18:0 were increased and the relative amounts of C18:1n-9 and C24:1n-9 were decreased in the livers of

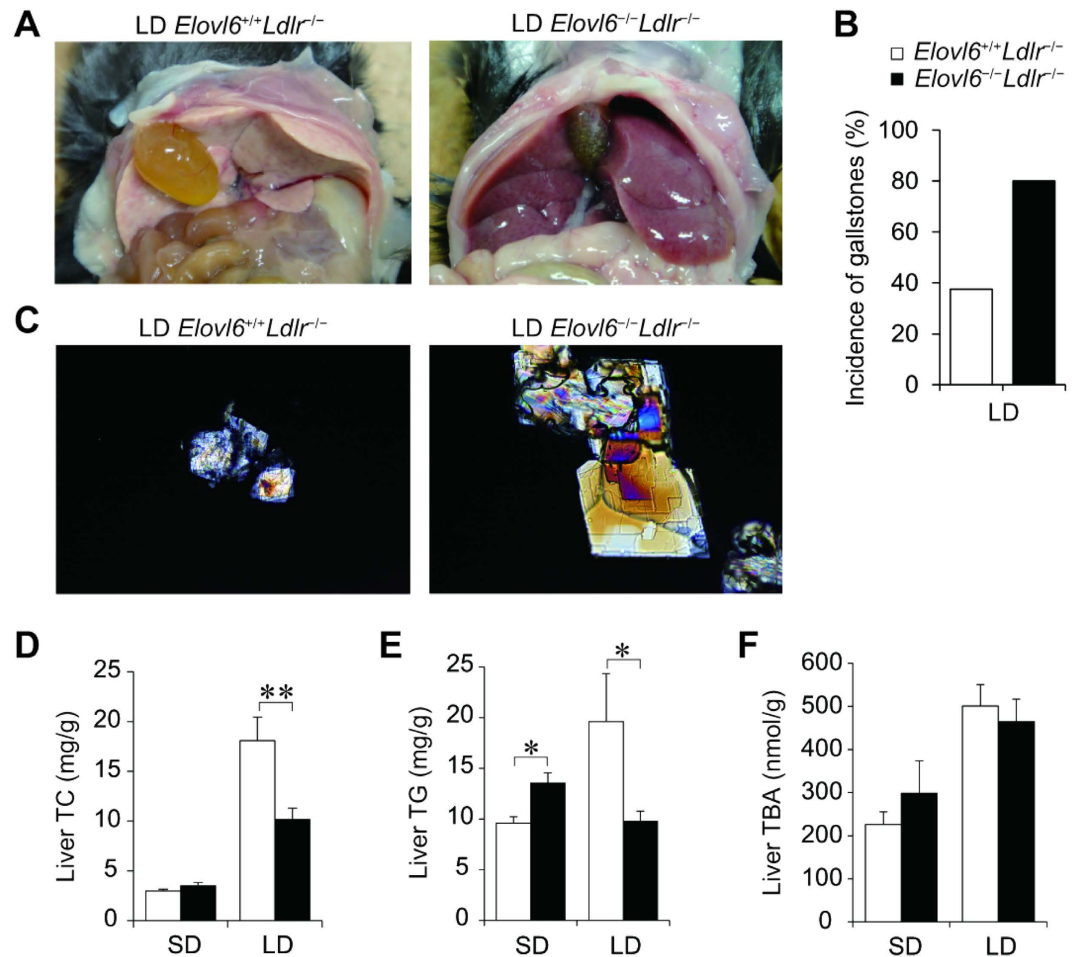


Figure 3. Elov6 deficiency suppresses lithogenic diet (LD)-induced hepatic lipid accumulation in *Ldlr*^{-/-} mice. (A) Representative photographs of livers from *Elov6*^{+/+}*Ldlr*^{-/-} and *Elov6*^{-/-}*Ldlr*^{-/-} mice fed an LD for 4 weeks. (B) The prevalence rate of gallstones in *Elov6*^{+/+}*Ldlr*^{-/-} and *Elov6*^{-/-}*Ldlr*^{-/-} mice fed an LD for 4 weeks (n = 8–10 per group). (C) Polarizing light microscopy of gallbladder bile from *Elov6*^{+/+}*Ldlr*^{-/-} and *Elov6*^{-/-}*Ldlr*^{-/-} mice fed an LD for 4 weeks (magnification, ×200). (D–F) Hepatic total cholesterol (TC) (D), triglyceride (TG) (E) and total bile acid (TBA) (F) levels in *Elov6*^{+/+}*Ldlr*^{-/-} and *Elov6*^{-/-}*Ldlr*^{-/-} mice fed a standard diet (SD) or an LD for 4 weeks (n = 8–13 per group). **P* < 0.05, ***P* < 0.01.

Elov6^{-/-}*Ldlr*^{-/-} mice compared with *Elov6*^{+/+}*Ldlr*^{-/-} mice. Despite different degrees of change depending on the lipid fraction, the overall changes in FA composition in both genotypes were consistent with Elov6 enzymatic activity.

Elov6 deficiency alters bile acid composition in the livers and bile of *Ldlr*^{-/-} mice. The composition of BAs is associated with hepatotoxicity and cholesterol crystallization^{24–27}. To investigate a potential role of Elov6 on BA metabolism and whether BA alterations could contribute to reduced LD-induced liver damage and gallstone formation in LD-fed *Elov6*^{-/-}*Ldlr*^{-/-} mice, the composition of individual BAs in the livers of *Elov6*^{+/+}*Ldlr*^{-/-} and *Elov6*^{-/-}*Ldlr*^{-/-} mice fed an SD or an LD were quantified by liquid chromatography/mass spectrometry (LC/MS) (see Supplementary Fig. S2 online). Determination of individual BA species revealed that taurocholic acid (TCA), tauro-β-muricholate (TβMCA) and tauro-ω-muricholate (TωMCA) represent the dominant BA species in SD-fed animals of both genotypes. The ablation of Elov6 in *Ldlr*^{-/-} mice had little effect on liver BA composition, except that the ratio of tauro-α-muricholate (TαMCA) was significantly decreased in the livers of *Elov6*^{-/-}*Ldlr*^{-/-} mice compared with *Elov6*^{+/+}*Ldlr*^{-/-} mice. Because of CA-overloading on the LD, there was a shift in the liver BA species in response to LD-feeding, with CA and its derivatives, TCA and taurodeoxycholic acid (TDCA), representing the major species in both genotypes. Elov6 deficiency significantly decreased the ratio of TDCA and TαMCA and significantly increased the ratio of glycocholic acid (GCA) in the livers of LD-fed *Ldlr*^{-/-} mice. TDCA is increased in NASH patients²⁶, providing a plausible biochemical explanation for the LD phenotype of *Elov6*^{-/-}*Ldlr*^{-/-} mice. Similar BA compositional changes were seen

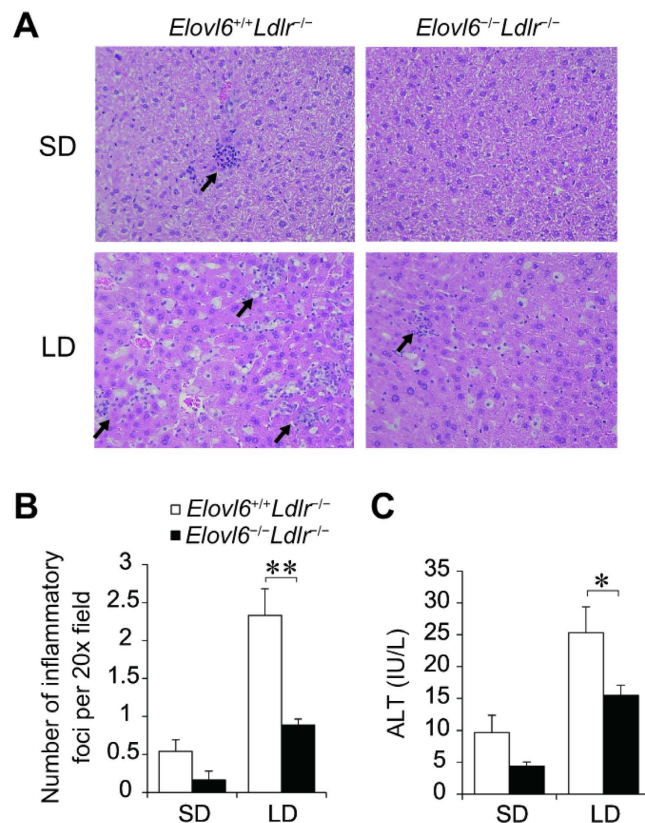


Figure 4. Attenuated hepatic inflammation and liver injury in lithogenic diet (LD)-fed *Elov6*^{-/-}*Ldlr*^{-/-} mice. (A) Representative hematoxylin and eosin (H&E)-stained sections of livers from *Elov6*^{+/+}*Ldlr*^{-/-} and *Elov6*^{-/-}*Ldlr*^{-/-} mice fed a standard diet (SD) or an LD for 4 weeks. (B) The number of inflammatory foci in H&E-stained sections from each animal at 20× magnification (n = 6–9 per group). (C) Plasma alanine aminotransferase (ALT) levels of *Elov6*^{+/+}*Ldlr*^{-/-} and *Elov6*^{-/-}*Ldlr*^{-/-} mice fed an SD or an LD for 4 weeks (n = 8–13 per group). **P* < 0.05, ***P* < 0.01.

in bile (see Supplementary Fig. S2 online). In contrast, lack of *Elov6* in *Ldlr*^{-/-} mice had little effect on BA composition in plasma despite strong suppression of the total BA level. However, lack of *Elov6* in *Ldlr*^{-/-} mice was associated with an increased concentration of chenodeoxycholic acid (CDCA) in an LD-fed state (see Supplementary Fig. S2 online).

***Elov6* deficiency alters LD-responsive gene expression in the livers of *Ldlr*^{-/-} mice.** To have some idea on the molecular mechanisms by which an LD results in such a striking phenotype in *Elov6*^{-/-}*Ldlr*^{-/-} mice, mRNA expression of candidate genes in livers from mice of both genotypes fed an SD or an LD diet was examined using quantitative real-time polymerase chain reaction (qPCR). Genes involved in FA synthesis controlled by sterol regulatory element binding protein 1c (*Srebf1c*), such as fatty acid synthase (*Fasn*), were significantly increased and stearoyl-CoA desaturase-1 (*Scd1*) showed a tendency to increase in the livers of LD-fed *Elov6*^{-/-}*Ldlr*^{-/-} mice compared with LD-fed *Elov6*^{+/+}*Ldlr*^{-/-} mice (Fig. 6A). Expression of genes involved in TG synthesis, including glycerol-3-phosphate acyltransferase (*Gpam*) and diacylglycerol O-acyltransferase 2 (*Dgat2*), was slightly increased in the livers of LD-fed *Elov6*^{-/-}*Ldlr*^{-/-} mice compared with LD-fed *Elov6*^{+/+}*Ldlr*^{-/-} mice; whereas, expression of diacylglycerol O-acyltransferase 1 (*Dgat1*) was similar in both genotypes. Expression of genes involved in cholesterol synthesis regulated by sterol regulatory element binding protein 2 (*Srebp2*), including 3-hydroxy-3- β -methylglutaryl-coenzyme A synthase 1 (*Hmgcs1*), was decreased, and expression of genes for cholesterol efflux enhanced by liver X receptor α (*Lxr α) (nuclear receptor subfamily 1, group H, member 3: *Nr1h3*), such as ATP-binding cassette sub-family A member 1 (*Abca1*), ATP-binding cassette sub-family G member 1 (*Abcg5*), and *Abcg8*, was increased in response to cholesterol feeding in both groups of mice (Fig. 6B). Expression of acetyl-coenzyme A acetyltransferase 2 (*Acat2*) was increased in LD-fed *Elov6*^{-/-}*Ldlr*^{-/-} mice compared with LD-fed *Elov6*^{+/+}*Ldlr*^{-/-} mice. The enhanced expression of lipogenic enzymes and *Acat2* in the livers of *Elov6*^{-/-}*Ldlr*^{-/-} mice might compensate for the unbalanced FA composition. Expression of carboxylesterase 3a and 3b (*Ces3a* and *Ces3b*) was suppressed by the LD in *Elov6*^{+/+}*Ldlr*^{-/-} mice, but was restored by the absence of *Elov6* (Fig. 6C).*

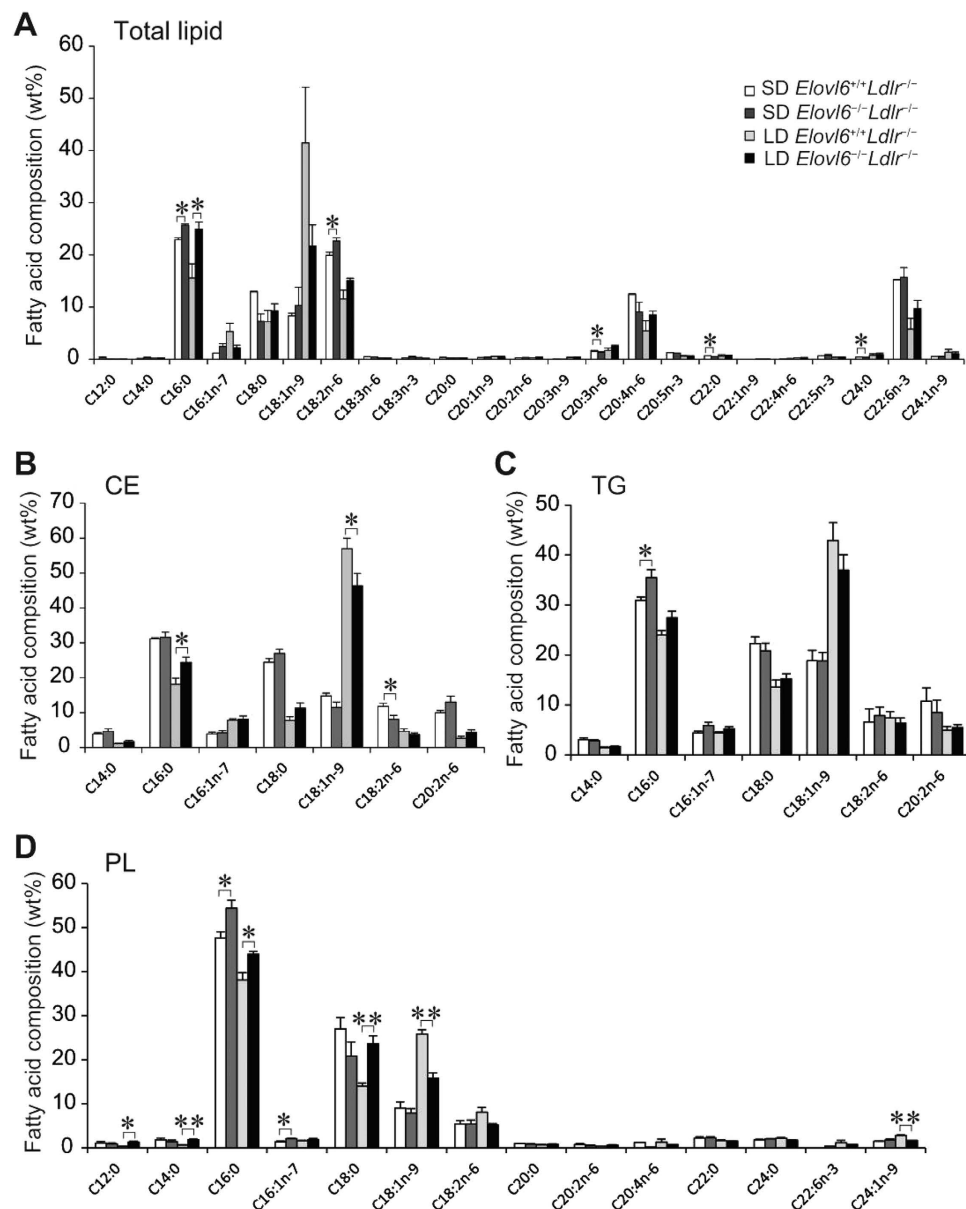


Figure 5. Hepatic fatty acid composition. (A) Hepatic fatty acid composition for total lipids, (B) the cholesterol ester (CE) fraction, (C) the triglyceride (TG) fraction and (D) the phospholipid (PL) fraction in livers from *Elov6*^{+/+}*Ldlr*^{-/-} and *Elov6*^{-/-}*Ldlr*^{-/-} mice fed a standard diet (SD) or a lithogenic diet (LD) for 4 weeks. Hepatic total lipids were extracted, and the major classes of lipids were separated on a silica column. The lipid fractions were methyl-esterified and quantified by gas chromatography (n = 3–6 per group). **P* < 0.05, ***P* < 0.01.

The expression of genes associated with BA metabolism was also examined (Fig. 7A). Loss of *Elov6* slightly decreased the expression of farnesoid X receptor (Fxr) (nuclear receptor subfamily 1, group H, member 4: *Nr1h4*) in mice on the SD but had little effect in the LD-fed mice. The LD increased the expression of the Fxr-target genes, liver receptor homolog-1 (*Lrh1*) (nuclear receptor subfamily 5, group A, member 2: *Nr5a2*) and small heterodimer partner (*Shp*) (nuclear receptor subfamily 0, group B, member 2: *Nr0b2*), in both genotypes. The biosynthesis of BAs in the liver is controlled by multiple cytochrome P450 (CYP) enzymes²⁸. The LD markedly suppressed mRNA expression of cholesterol 7 α -hydroxylase (*Cyp7a1*) and sterol 12 α -hydroxylase (*Cyp8b1*), the two key enzymes in BA synthesis, in both genotypes. Expression of sterol 27-hydroxylase (*Cyp27a1*) and oxysterol 7 α -hydroxylase (*Cyp7b1*), which are involved in an alternative pathway of BA synthesis, was also decreased by the LD in *Elov6*^{+/+}*Ldlr*^{-/-} mice, but was significantly upregulated in the livers of LD-fed *Elov6*^{-/-}*Ldlr*^{-/-} mice compared with LD-fed *Elov6*^{+/+}*Ldlr*^{-/-} mice. Expression of solute carrier family 10 member 1 (*Slc10a1*) and solute carrier organic anion transporter family member 1a1 (*Slco1a1*), which are involved in BA uptake by

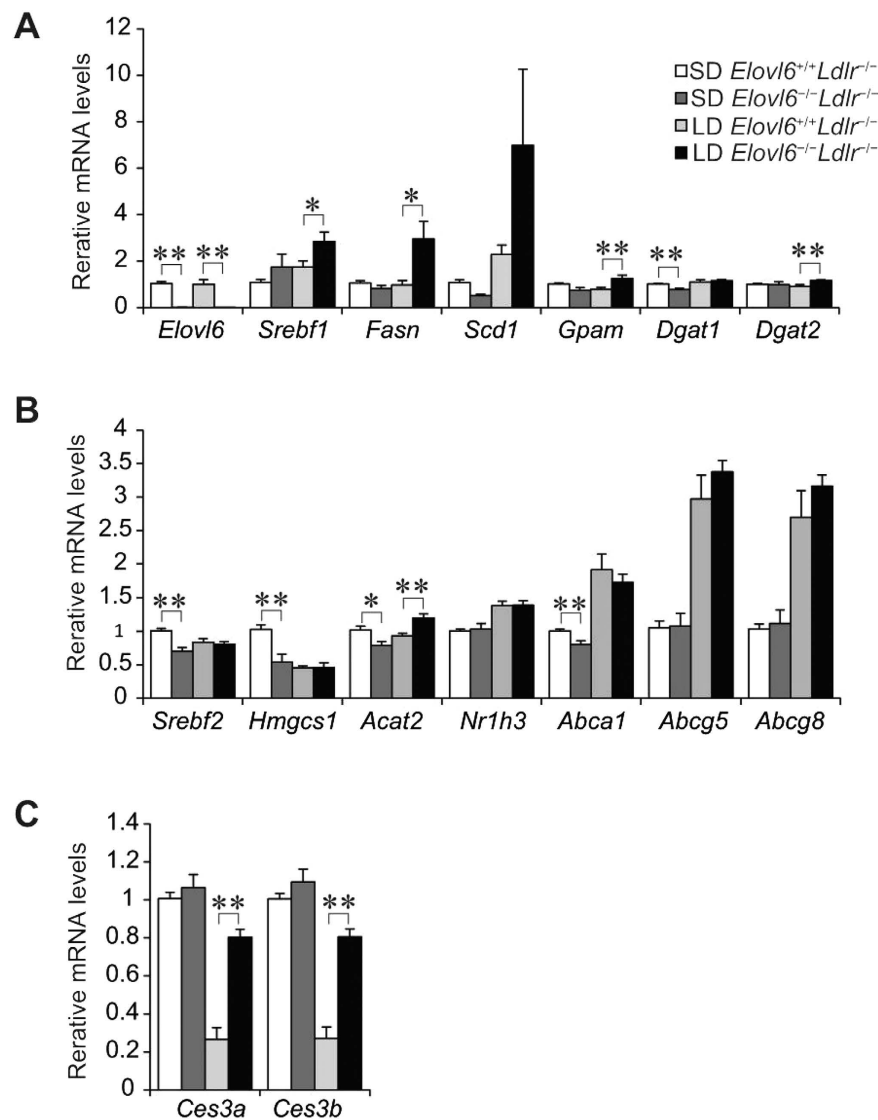


Figure 6. Quantitative real-time PCR (qPCR) analysis of genes involved in steatohepatitis.

Elovl6^{+/+}*Ldlr*^{-/-} and *Elovl6*^{-/-}*Ldlr*^{-/-} mice were fed a standard diet (SD) or a lithogenic diet (LD) for 4 weeks and sacrificed following 4 h of food deprivation (n = 8–13 per group). (A) qPCR analysis of genes for fatty acid and triglyceride synthesis, (B) cholesterol metabolism and (C) carboxylesterase. **P* < 0.05, ***P* < 0.01.

hepatocytes, was suppressed by the LD in *Elovl6*^{+/+}*Ldlr*^{-/-} mice. Strikingly, LD-fed *Elovl6*^{-/-}*Ldlr*^{-/-} mice displayed a complete lack of *Slc10a1* and *Slco1a1* suppression. Expression of ATP-binding cassette sub-family B member 11 (*Abcb11*), an ABC transporter responsible for the transport of bile salt from hepatocytes into the bile, was significantly upregulated in the livers by the LD with greater intensity in *Elovl6*^{-/-}*Ldlr*^{-/-} mice compared to LD *Elovl6*^{+/+}*Ldlr*^{-/-} mice. Expression of ATP-binding cassette subfamily C member 1 (*Abcc1*), *Abcc3* and *Abcc4*, which are involved in basolateral BA excretion, was markedly elevated in LD-fed *Elovl6*^{+/+}*Ldlr*^{-/-} mice. The expression of *Abcc1* was significantly decreased, and *Abcc4* tended to decrease (*P* = 0.059) in LD-fed *Elovl6*^{-/-}*Ldlr*^{-/-} mice compared with LD-fed *Elovl6*^{+/+}*Ldlr*^{-/-} mice. Consistently with mRNA levels, hepatic CYP7A1 protein was suppressed by LD feeding in both genotypes (Fig. 7B). Hepatic protein levels of CYP27a1 and SLC10A1 was also decreased by the LD in *Elovl6*^{+/+}*Ldlr*^{-/-} mice, but was upregulated in LD-fed *Elovl6*^{-/-}*Ldlr*^{-/-} mice compared with LD-fed *Elovl6*^{+/+}*Ldlr*^{-/-} mice.

The expression of genes involved in BA homeostasis in ileum was also examined (Supplementary Fig. S3). The expression levels of *Nr1h4*, solute carrier family 10 member 2 (*Slc10a2*), *Abcc2*, fatty acid binding protein 6 ileal (*Fabp6*), solute carrier family 51 beta subunit (*Slc51b*) and fibroblast growth factor 15 (*Fgf15*) were similar between LD-fed *Elovl6*^{+/+}*Ldlr*^{-/-} and LD-fed *Elovl6*^{-/-}*Ldlr*^{-/-} mice.

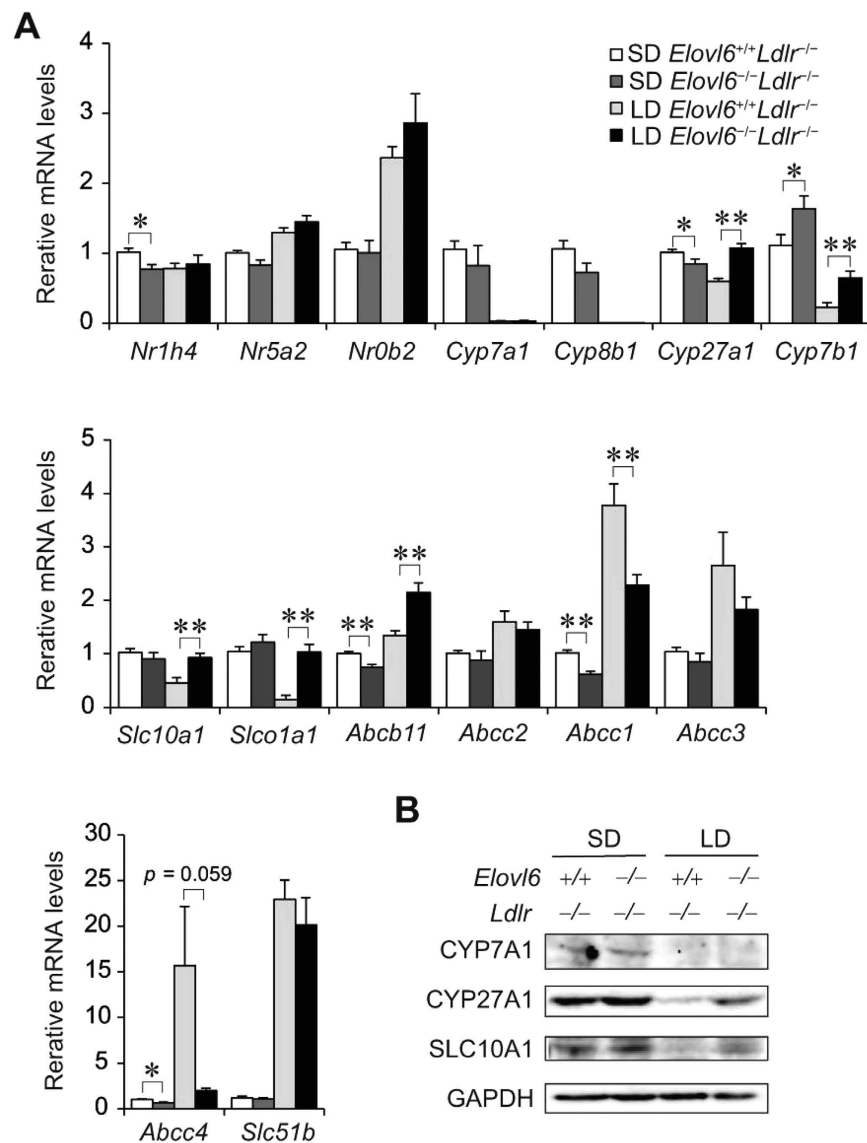


Figure 7. Hepatic expression levels of genes involved in BA metabolism. *Elov6*^{+/+}*Ldlr*^{-/-} and *Elov6*^{-/-}*Ldlr*^{-/-} mice were fed a standard diet (SD) or a lithogenic diet (LD) for 4 weeks and sacrificed following 4 h of food deprivation (n = 8–13 per group). (A) qPCR analysis of genes for BA metabolism. * $P < 0.05$, ** $P < 0.01$. (B) Immunoblot analysis of CYP7A1, CYP27A1, SLC10A1 and glyceraldehyde 3-phosphate dehydrogenase (GAPDH) in the livers of *Elov6*^{+/+}*Ldlr*^{-/-} and *Elov6*^{-/-}*Ldlr*^{-/-} mice fed a SD or a LD for 4 weeks.

***Elov6* deletion attenuates the inflammatory response and hepatic injury in LD-fed *Ldlr*^{-/-} mice.** Hepatic damage in LD-fed *Ldlr*^{-/-} mice is associated with hepatic inflammation, oxidative stress and fibrosis. In agreement with histological and metabolic observations (Fig. 4), inflammatory response genes including tumour necrosis factor α (*Tnf α*), interleukin 1 β (*Il-1b*), toll-like receptor 4 (*Tlr4*), CD14 antigen (*Cd14*) and secreted phosphoprotein 1 (*Spp1*) were upregulated in the livers of LD-fed *Elov6*^{+/+}*Ldlr*^{-/-} mice (Fig. 8A). However, induction of these genes showed marked or a trend to suppression in LD-fed *Elov6*^{-/-}*Ldlr*^{-/-} mice. The expression levels of genes for the nicotinamide adenine dinucleotide phosphate (NADPH) oxidase complex, neutrophil cytosolic factor 1 (*Ncf1*), neutrophil cytosolic factor 2 (*Ncf2*) and cytochrome b-245 beta polypeptide (*Cybb*), were upregulated in LD-fed *Elov6*^{+/+}*Ldlr*^{-/-} mice, but significantly decreased in LD-fed *Elov6*^{-/-}*Ldlr*^{-/-} mice compared with LD-fed *Elov6*^{+/+}*Ldlr*^{-/-} mice (Fig. 8B). The expression level of the gene for transforming growth factor β 1 (*Tgfb1*) was upregulated in LD-fed *Elov6*^{+/+}*Ldlr*^{-/-} mice but suppressed in LD-fed *Elov6*^{-/-}*Ldlr*^{-/-} mice compared with LD-fed *Elov6*^{+/+}*Ldlr*^{-/-} mice (Fig. 8C). Decreased hepatic inflammation, oxidative stress and fibrosis in *Elov6*^{-/-}*Ldlr*^{-/-} mice were further examined by measuring stresses and proinflammatory pathways. *Elov6* deficiency significantly attenuated LD-induced c-Jun N-terminal kinase (JNK) activation and α -smooth muscle actin (α -SMA) levels in *Ldlr*^{-/-} mice (Fig. 8D,E).

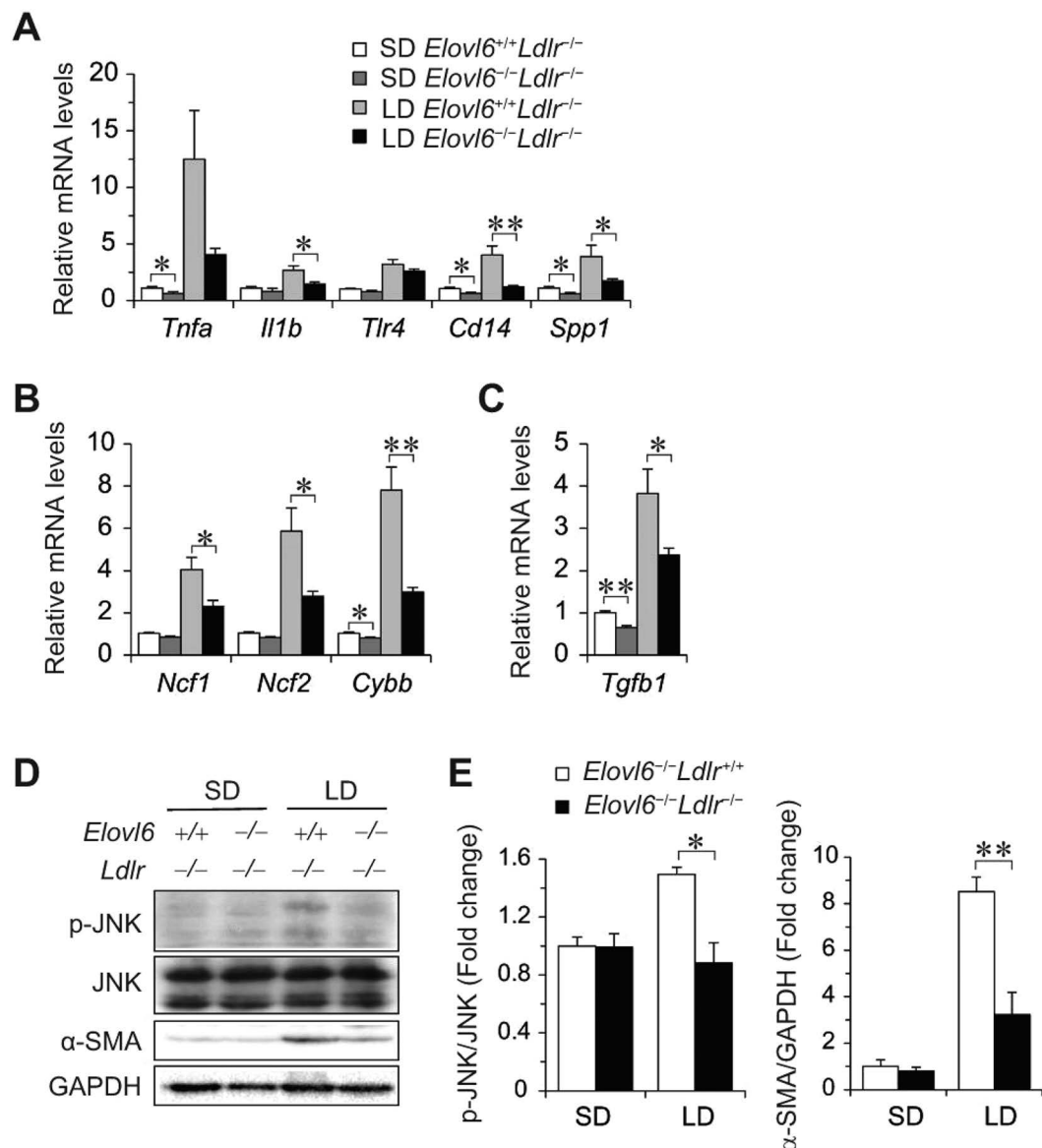


Figure 8. Effects of *Elov6* deficiency on hepatic mRNA and levels of proteins involved in inflammation, oxidative stress and fibrosis. (A–C) Quantitative real-time PCR (qPCR) analysis of genes for inflammation (A), reactive oxygen species (ROS) generation (B) and fibrogenesis (C). (D) Immunoblot analysis of phosphorylated and total anti-phospho-c-Jun N-terminal kinase (JNK), α -smooth muscle actin (α -SMA) and GAPDH in the livers of *Elov6*^{+/+}*Ldlr*^{-/-} and *Elov6*^{-/-}*Ldlr*^{-/-} mice fed a standard diet (SD) or a lithogenic diet (LD) for 4 weeks. (E) Ratio between phosphorylated and total JNK and α -SMA and GAPDH on densitometry analysis (n = 2–4 per group). **P* < 0.05, ***P* < 0.01.

Discussion

Our current findings show that the absence of the *Elov6* gene product strongly inhibits LD-induced accumulation of hepatic and plasma cholesterol and plasma TBA in *Ldlr*^{-/-} mice. The absence of *Elov6* also imparts striking protection from LD-induced hepatic injury by ameliorating hepatic inflammation, oxidative stress and stellate cell activation. The net results of these complex adaptations are a striking decrease in susceptibility to NASH, but increased susceptibility to gallstones. Normolipidemic *Elov6* deficient mice are known to be protected from AHF-induced NASH with no change in hepatic lipid content or profiles²³. We have now extended the findings in *Elov6*^{-/-} mice to include protection from diet-induced hepatosteatosis and inflammation in dyslipidemic LDLR-deficient mice.

Feeding an LD (cholesterol and CA loading) causes accumulation of plasma, hepatic and bile cholesterol in *Ldlr*^{-/-} mice in response to activation of both LXR and FXR pathways and suppression of SREBP-2. Plasma and hepatic BAs were also elevated despite adaptive responses to hepatic handling of BA, such as decreased hepatic uptake, increased basolateral excretion and enhanced excretion into bile,

as evidenced by changes in gene expression of BA transporters and pumps to prevent overaccumulation of BA in hepatocytes (as schematized in Supplementary Fig. S4). Meanwhile, the absence of *Elovl6* ameliorated LD-induced accumulation of lipids and BA in *Ldlr*^{-/-} mice, indicating that *Elovl6* and FA composition play a role in cholesterol and BA handling in hepatocytes.

A potential mechanism for the reduction in hepatic and plasma cholesterol in LD-fed *Elovl6*^{-/-}*Ldlr*^{-/-} mice is the suppression of esterification of cholesterol secondary to decreased oleate (C18:1) levels in the liver. *Elovl6* deficiency significantly reduced oleate levels in CE and PL fractions. Because oleate, the major esterified cholesterol in liver, is a better substrate for ACAT than palmitate, inhibition of the conversion from palmitate to stearate resulting in decreased endogenous monounsaturated FAs could lead to reduction in esterified cholesterol. Expression of *Ces3a* and *Ces3b* was strongly suppressed by the LD in *Elovl6*^{+/+}*Ldlr*^{-/-} mice and restored in *Elovl6*^{-/-}*Ldlr*^{-/-} mice. Esterase and lipase activities of these genes might contribute to decreased hepatic lipid content in LD-fed *Elovl6*^{-/-}*Ldlr*^{-/-} mice. Our data are consistent with previous studies showing that mice harbouring a natural mutation in the *Scd1* gene are deficient in hepatic CE and TG with decreased monounsaturated FAs (C16:1 and C18:1), and indicate that a reduction in hepatic oleate is likely to be a major contributor to decreased hepatic and plasma cholesterol^{29,30}. It has also been reported that monounsaturated FA-containing CE levels were markedly elevated in the livers of mice fed a cholate-supplemented high-fat diet, but without an increase in the level of TG or PL in the liver, coupled with the biological and histological features of fatty liver injury³¹. Moreover, increased oleate levels have been found in the livers of NASH patients³². Recent publications have also indicated that hepatic cholesterol accumulation is more toxic than TG accumulation and may be a trigger for the progression of NAFLD^{13,33,34}. Therefore, these data indicate that the excessive accumulation of CE with oleate might contribute to liver injury and that consequent loss of oleate resulting from the absence of *Elovl6* could be the cause of the amelioration in the current study.

Our data are consistent with our recent study using an AHF diet-fed mouse model of NAFLD/NASH, which demonstrated a critical role for *Elovl6* in disease pathogenesis²³. In that study, *Elovl6*^{-/-} mice displayed a significant decrease in hepatic inflammation, oxidative stress, liver injury and fibrosis, but without amelioration of hepatosteatosis. The finding of protection against steatosis in the present study, which is in contrast to the previous study, is presumably because the current study protocol highlights cholesterol rather than TG accumulation in hepatosteatosis. LDLR deficiency activates cholesterol synthesis in the liver. In addition, the LD has a lower FA content than the AHF diet. Therefore, in an LD-fed *Ldlr*^{-/-} mouse model, the reduction of oleate by *Elovl6* deficiency is further reflected in CE formation. Our previous study also showed a reduction in esterified cholesterol accumulation in macrophages from *Elovl6*^{-/-} mice¹⁸.

One of the intriguing findings of the present study was the protection against LD-induced serum BA elevation coupled with altered expression of genes involved in hepatic BA metabolism (*Cyp27a1*, *Cyp7b1*, *Slc10a1*, *Slco1a1*, *Abcb11* and *Abcc1*) in LD-fed *Elovl6*^{-/-}*Ldlr*^{-/-} mice. *Cyp27a1* and *Cyp7b1* expression were significantly increased in the livers of *Elovl6*^{-/-}*Ldlr*^{-/-} mice compared with *Elovl6*^{+/+}*Ldlr*^{-/-} mice fed on both an SD and an LD. The alternative pathway may contribute very little to overall BA synthesis under normal conditions, but may become more predominant in the presence of liver disease and may compensate for the limitations in the classical pathway^{35,36}. Increased *Cyp27a1* and *Cyp7b1* mRNA levels are indicative of a functional upregulation of the alternative pathway to reduce hepatotoxicity and the progression of liver disease to NASH³⁷. In addition, *Cyp7b1* expression was negatively associated with hepatic steatosis in an animal model³⁸. Therefore, the increase in hepatic *Cyp7b1* expression might contribute to the suppression of hepatosteatosis and liver injury in LD-fed *Elovl6*^{-/-}*Ldlr*^{-/-} mice. In the present study, the expression of *Slc10a1* and *Slco1a1* was increased in LD-fed *Elovl6*^{-/-}*Ldlr*^{-/-} mice in concert with decreased expression of *Abcc1* and *Abcc4*. In support of these observations, increases in serum BAs were related to a decrease and an increase in *Slco1a1* and *Abcc4* expression, respectively, in the livers of mouse NASH models³⁹. These data suggest that LD-fed *Elovl6*^{-/-}*Ldlr*^{-/-} mice have a greater ability to remove BAs from the hepatic-portal circulation than LD-fed *Elovl6*^{+/+}*Ldlr*^{-/-} mice.

In the present study, the LD significantly decreased the expression of *Slc10a1* and *Slco1a1* and increased the expression of *Abcc1* and *Abcc4* in the livers of *Elovl6*^{+/+}*Ldlr*^{-/-} mice, whereas the expression of these genes remained unchanged in LD-fed *Elovl6*^{-/-}*Ldlr*^{-/-} mice. It is well known that inflammatory signals act as potent regulators of the expression of sinusoidal and basolateral BA transporters. For example, lipopolysaccharide (LPS) downregulates the expression of *Slc10a1* and *Slco1a1* and increases the expression of *Abcc1*⁴⁰. In addition, depletion of Kupffer cells inhibits the LPS-induced downregulation of *Slco1a1* and upregulation of *Abcc4* by attenuating the increase in TNF- α expression^{41,42}. These previous observations support the present results and demonstrate one of the mechanisms by which inflammatory signals disrupt BA homeostasis in the liver. Because *Elovl6* deficiency or modification of FA composition causes a drastic change in cholesterol metabolism, *Elovl6* might also regulate BA handling (hepatic production, uptake, basolateral and canalicular excretion) in the enterohepatic circulation, although the detailed molecular mechanism is unknown.

The current findings demonstrate that LD-fed *Elovl6*^{-/-}*Ldlr*^{-/-} mice are more susceptible to gallstone formation as a result of an alteration in hepatic cholesterol metabolism that promotes hepatic free cholesterol secretion into bile, coupled with alterations in hepatic BA metabolism. The net result of these complex adaptations is a striking increase in the formation of cholesterol crystals. In the gallbladder bile, the solubility of cholesterol is maintained by the balance among cholesterol, bile salts and phospholipids^{27,43}.

The increased biliary concentration of cholesterol in *Elovl6*^{-/-}*Ldlr*^{-/-} mice resulted in supersaturation, precipitation and crystallization of cholesterol. The FA compositional changes in the PL fraction might also affect the susceptibility of LD-fed *Elovl6*^{-/-}*Ldlr*^{-/-} mice to gallstones. Several of these conclusions and their underlying mechanisms warrant further examination.

In conclusion, this study demonstrates that *Elovl6* plays a crucial role in the development and progression of steatohepatitis through the regulation of FA, cholesterol and BA metabolism. These findings are an important step forward in understanding the pathophysiology of NASH and the contribution and interaction of *Elovl6* in hepatic inflammation associated with hepatic lipid accumulation. Further studies are needed to determine the exact contribution of *Elovl6* to the risk of developing NASH and may provide a basis for the development of alternative therapeutic strategies and markers for diagnostic tests.

Methods

Animals and diets. *Elovl6*^{-/-} mice (C57BL/6 background) were generated as described previously¹⁶. *Ldlr*^{-/-} mice (C57BL/6J background) were purchased from the Jackson Laboratory. *Elovl6*^{-/-} mice were crossed with *Ldlr*^{-/-} mice to produce *Elovl6*^{-/-}*Ldlr*^{-/-} mice. The mice were housed in a pathogen-free barrier facility with a 12 h light/dark cycle and were given free access to food and water. Beginning at 11–16 weeks of age, mice were fed either a standard laboratory rodent chow diet (SD) (MF; Oriental Yeast, Tokyo, Japan) or an LD (16.5% fat, 1.25% cholesterol, 0.5% cholic acid (CA); F2HFD1; Oriental Yeast) for 4 weeks [n = 13 *Ldlr*^{-/-} mice fed SD (n = 5 of 11-week-old and n = 8 of 16-weeks-old), n = 8 *Elovl6*^{-/-}*Ldlr*^{-/-} mice fed SD (n = 3 of 11-week-old and n = 5 of 16-week-old), n = 12 *Ldlr*^{-/-} mice fed LD (n = 5 of 11-week-old and n = 7 of 16-weeks-old), and n = 13 *Elovl6*^{-/-}*Ldlr*^{-/-} mice fed LD (n = 6 of 11-week-old and n = 7 of 16-week-old)]. Details of the LD are shown in Table S1 online. Age-matched male mice were used for all experiments. Mice were sacrificed during the light phase after food deprivation for 4 h. Plasma samples were collected from the post-orbital plexus. Tissues were isolated immediately, weighed and stored in liquid nitrogen. All animal husbandry and animal experiments complied with the guidelines of the University of Tsukuba's Regulations of Animal Experiments and were approved by the Animal Experiment Committee of the University of Tsukuba.

Plasma analysis. Plasma TC, TG, TBA and ALT were determined using commercially available assay kits (Wako Pure Chemicals, Tokyo, Japan). For the lipoprotein distribution analysis, plasma samples were analysed using an upgraded HPLC technique as previously described (Skylight Biotech Inc., Akita, Japan)⁴⁴.

Gallbladder bile and gallstone analysis. After 4 h fasting, animals were sacrificed and cholecystectomies were performed. The gallbladder was punched at the fundus to collect gallbladder bile. Bile samples were collected and immediately analysed by polarizing light microscopy for the presence of cholesterol monohydrate crystals.

Hepatic lipid analysis. Total lipids were extracted from liver tissues using Folch solution (chloroform-methanol, 2:1 v/v)⁴⁵, dried and dissolved in 2-propanol. Hepatic lipid extracts were assayed for TC and TG levels using commercial assay kits for blood cholesterol and TG determination (Wako Pure Chemicals).

Hepatic total bile acid analysis. Hepatic TBAs were extracted from frozen tissue by homogenization in 75% ethanol and incubation at 50 °C for 2 h as previously described⁴⁶. The extracted supernatants were assayed using a commercially available assay kit (Wako Pure Chemicals).

Fatty acid composition of liver. Total lipids in liver were extracted using Bligh–Dyer's procedure⁴⁷, and TG and esterified cholesterol were separated on 500 mg silica columns (Supelclean PSA SPE Tube; Sigma-Aldrich Japan, Tokyo, Japan). The lipid fractions in each sample were methyl-esterified and the relative abundance of each FA was quantified by gas chromatography (SRL, Inc., Tokyo, Japan)⁴⁸.

Histology. Livers were removed, fixed in 10% neutral buffered formalin, embedded in paraffin and cut into 4-μm-thick sections for subsequent H&E staining.

RNA extraction and quantitative real-time PCR. Total RNA was extracted from livers using Sepasol reagent (Nacalai Tesque, Kyoto, Japan) and was reverse-transcribed using the PrimeScript RT Master kit (Takara Bio Inc., Shiga, Japan) according to the manufacturer's protocols. qPCR was performed using SYBR Premix Ex Taq (Takara Bio Inc.) and specific primer sets with the Thermal Cycler Dice Real Time System Single (Takara Bio Inc.). Primer sequences for *Acat2*, *Nr1h3*, *Ces3a*, *Ces3b*, *Nr1h4*, *Nr5a2*, *Nr0b2*, *Cyp7a1*, *Cyp8b1*, *Cyp27a1*, *Cyp7b1*, *Slc10a1*, *Slco1a1*, *Abcb11*, *Abcc2*, *Abcc1*, *Abcc3*, *Abcc4*, *Slc51b*, *Cd14* and *Cybb* are summarized in Supplementary Table S2 online. Other qPCR primers used have been described previously^{16,23,49}. The expression levels of mRNA were normalized to those of peptidylprolyl isomerase A (*Ppia*) mRNA.

Immunoblotting. Immunoblotting was performed as described previously¹⁶. Protein isolated from whole livers was loaded onto 10% sodium dodecyl-sulphate polyacrylamide gel electrophoresis gels and transferred to polyvinylidene difluoride membranes (Millipore). The membranes were probed with anti-CYP7A1 (Santa Cruz Biotechnology, Dallas, TX), CYP27A1, SLC10A1, α -SMA (Abcam, Cambridge, UK) and phospho-JNK, JNK, glyceraldehyde 3-phosphate dehydrogenase (GAPDH) (Cell Signaling Technology, Denver, MA), followed by horseradish peroxidase-conjugated anti-mouse or rabbit IgG (Cell Signaling Technology). Immune complexes were visualized using enhanced chemiluminescence (GE Healthcare).

Statistical analysis. Results are expressed as mean \pm SEM. Data between groups were analysed by Student's *t*-test. Differences were considered significant at $P < 0.05$.

References

- Lazo, M. & Clark, J. M. The epidemiology of nonalcoholic fatty liver disease: a global perspective. *Semin. Liver. Dis.* **28**, 339–350 (2008).
- Argo, C. K. & Caldwell, S. H. Epidemiology and natural history of non-alcoholic steatohepatitis. *Clin. Liver. Dis.* **13**, 511–531 (2009).
- Everhart, J. E. & Bambha, K. M. Fatty liver: think globally. *Hepatology* **51**, 1491–1493 (2010).
- Cohen, J. C., Horton, J. D. & Hobbs, H. H. Human fatty liver disease: old questions and new insights. *Science* **332**, 1519–1523 (2011).
- Day, C. P. & James, O. F. Steatohepatitis: a tale of two “hits”? *Gastroenterology* **114**, 842–845 (1998).
- Neuschwander-Tetri, B. A. Hepatic lipotoxicity and the pathogenesis of nonalcoholic steatohepatitis: the central role of nontriglyceride fatty acid metabolites. *Hepatology* **52**, 774–788 (2010).
- Tilg, H. & Moschen, A. R. Evolution of inflammation in nonalcoholic fatty liver disease: the multiple parallel hits hypothesis. *Hepatology* **52**, 1836–1846 (2010).
- Sarwar, N. *et al.* Triglyceride-mediated pathways and coronary disease: collaborative analysis of 101 studies. *Lancet* **375**, 1634–1639 (2010).
- Yamaguchi, K. *et al.* Inhibiting triglyceride synthesis improves hepatic steatosis but exacerbates liver damage and fibrosis in obese mice with nonalcoholic steatohepatitis. *Hepatology* **45**, 1366–1374 (2007).
- Amaro, A. *et al.* Dissociation between intrahepatic triglyceride content and insulin resistance in familial hypobetalipoproteinemia. *Gastroenterology* **139**, 149–153 (2010).
- Musso, G. *et al.* Dietary habits and their relations to insulin resistance and postprandial lipemia in nonalcoholic steatohepatitis. *Hepatology* **37**, 909–916 (2003).
- Yasutake, K. *et al.* Nutritional investigation of non-obese patients with non-alcoholic fatty liver disease: the significance of dietary cholesterol. *Scand. J. Gastroenterol.* **44**, 471–477 (2009).
- Mari, M. *et al.* Mitochondrial free cholesterol loading sensitizes to TNF- and Fas-mediated steatohepatitis. *Cell Metab.* **4**, 185–198 (2006).
- Moon, Y. A., Shah, N. A., Mohapatra, S., Warrington, J. A. & Horton, J. D. Identification of a mammalian long chain fatty acyl elongase regulated by sterol regulatory element-binding proteins. *J. Biol. Chem.* **276**, 45358–45366 (2001).
- Matsuzaka, T. *et al.* Cloning and characterization of a mammalian fatty acyl-CoA elongase as a lipogenic enzyme regulated by SREBPs. *J. Lipid Res.* **43**, 911–920 (2002).
- Matsuzaka, T. *et al.* Crucial role of a long-chain fatty acid elongase, Elov6, in obesity-induced insulin resistance. *Nat. Med.* **13**, 1193–1202 (2007).
- Tang, N. *et al.* Ablation of Elov6 protects pancreatic islets from high-fat diet-induced impairment of insulin secretion. *Biochem. Biophys. Res. Commun.* **450**, 318–323 (2014).
- Saito, R. *et al.* Macrophage Elov6 deficiency ameliorates foam cell formation and reduces atherosclerosis in low-density lipoprotein receptor-deficient mice. *Arterioscler. Thromb. Vasc. Biol.* **31**, 1973–1979 (2011).
- Wouters, K. *et al.* Dietary cholesterol, rather than liver steatosis, leads to hepatic inflammation in hyperlipidemic mouse models of nonalcoholic steatohepatitis. *Hepatology* **48**, 474–486 (2008).
- Bieghs, V. *et al.* LDL receptor knock-out mice are a physiological model particularly vulnerable to study the onset of inflammation in non-alcoholic fatty liver disease. *PLoS one* **7**, e30668 (2012).
- Depner, C. M., Philbrick, K. A. & Jump, D. B. Docosahexaenoic acid attenuates hepatic inflammation, oxidative stress, and fibrosis without decreasing hepatosteatosis in a Ldlr(-/-) mouse model of western diet-induced nonalcoholic steatohepatitis. *J. Nutr.* **143**, 315–323 (2013).
- Ishibashi, S. *et al.* Hypercholesterolemia in low density lipoprotein receptor knockout mice and its reversal by adenovirus-mediated gene delivery. *J. Clin. Invest.* **92**, 883–893 (1993).
- Matsuzaka, T. *et al.* Elov6 promotes nonalcoholic steatohepatitis. *Hepatology* **56**, 2199–2208 (2012).
- Allen, K., Jaeschke, H. & Copple, B. L. Bile acids induce inflammatory genes in hepatocytes: a novel mechanism of inflammation during obstructive cholestasis. *Am. J. Pathol.* **178**, 175–186 (2011).
- Zhang, Y. *et al.* Effect of bile duct ligation on bile acid composition in mouse serum and liver. *Liver Int.* **32**, 58–69 (2012).
- Lake, A. D. *et al.* Decreased hepatotoxic bile acid composition and altered synthesis in progressive human nonalcoholic fatty liver disease. *Toxicol. Appl. Pharmacol.* **268**, 132–140 (2013).
- Moschetta, A., VanBerge-Henegouwen, G. P., Portincasa, P., Palasciano, G. & Van Erpecum, K. J. Cholesterol crystallization in model bile: effects of bile salt and phospholipid species composition. *J. Lipid Res.* **42**, 1273–1281 (2001).
- Russell, D. W. The enzymes, regulation, and genetics of bile acid synthesis. *Annu. Rev. Biochem.* **72**, 137–174 (2003).
- Miyazaki, M., Kim, Y. C., Gray-Keller, M. P., Attie, A. D. & Ntambi, J. M. The biosynthesis of hepatic cholesterol esters and triglycerides is impaired in mice with a disruption of the gene for stearoyl-CoA desaturase 1. *J. Biol. Chem.* **275**, 30132–30138 (2000).
- MacDonald, M. L. *et al.* Absence of stearoyl-CoA desaturase-1 ameliorates features of the metabolic syndrome in LDLR-deficient mice. *J. Lipid Res.* **49**, 217–229 (2008).
- Watanabe, S. & Tsuneyama, K. Cattle bile but not bear bile or pig bile induces lipid profile changes and fatty liver injury in mice: mediation by cholic acid. *J. Toxicol. Sci.* **37**, 105–121 (2012).
- Allard, J. P. *et al.* Nutritional assessment and hepatic fatty acid composition in non-alcoholic fatty liver disease (NAFLD): a cross-sectional study. *J. Hepatol.* **48**, 300–307 (2008).
- Wouters, K. *et al.* Intrahepatic cholesterol influences progression, inhibition and reversal of non-alcoholic steatohepatitis in hyperlipidemic mice. *FEBS Lett.* **584**, 1001–1005 (2010).

34. Zhao, L. *et al.* Inflammatory stress exacerbates hepatic cholesterol accumulation via increasing cholesterol uptake and de novo synthesis. *J. Gastroenterol. Hepatol.* **26**, 875–883 (2011).
35. Chawla, A., Repa, J. J., Evans, R. M. & Mangelsdorf, D. J. Nuclear receptors and lipid physiology: opening the X-files. *Science* **294**, 1866–1870 (2001).
36. Crosignani, A. *et al.* Changes in classic and alternative pathways of bile acid synthesis in chronic liver disease. *Clin. Chim. Acta.* **382**, 82–88 (2007).
37. Beilke, L. D. *et al.* Constitutive androstane receptor-mediated changes in bile acid composition contributes to hepatoprotection from lithocholic acid-induced liver injury in mice. *Drug Metab. Dispos.* **37**, 1035–1045 (2009).
38. Guillen, N. *et al.* Microarray analysis of hepatic gene expression identifies new genes involved in steatotic liver. *Physiol. Genomics* **37**, 187–198 (2009).
39. Tanaka, N., Matsubara, T., Krausz, K. W., Patterson, A. D. & Gonzalez, F. J. Disruption of phospholipid and bile acid homeostasis in mice with nonalcoholic steatohepatitis. *Hepatology* **56**, 118–129 (2012).
40. Cherrington, N. J., Slitt, A. L., Li, N. & Klaassen, C. D. Lipopolysaccharide-mediated regulation of hepatic transporter mRNA levels in rats. *Drug Metab. Dispos.* **32**, 734–741 (2004).
41. Sturm, E. *et al.* Kupffer cell depletion with liposomal clodronate prevents suppression of Ntcp expression in endotoxin-treated rats. *J. Hepatol.* **42**, 102–109 (2005).
42. Campion, S. N. *et al.* Hepatic Mrp4 induction following acetaminophen exposure is dependent on Kupffer cell function. *Am. J. Physiol. Gastrointest. Liver Physiol.* **295**, G294–304 (2008).
43. Wang, D. Q. & Carey, M. C. Complete mapping of crystallization pathways during cholesterol precipitation from model bile: influence of physical-chemical variables of pathophysiologic relevance and identification of a stable liquid crystalline state in cold, dilute and hydrophilic bile salt-containing systems. *J. Lipid Res.* **37**, 606–630 (1996).
44. Usui, S., Hara, Y., Hosaki, S. & Okazaki, M. A new on-line dual enzymatic method for simultaneous quantification of cholesterol and triglycerides in lipoproteins by HPLC. *J. Lipid Res.* **43**, 805–814 (2002).
45. Folch, J., Lees, M. & Sloane Stanley, G. H. A simple method for the isolation and purification of total lipides from animal tissues. *J. Biol. Chem.* **226**, 497–509 (1957).
46. Ma, K. *et al.* Circadian dysregulation disrupts bile acid homeostasis. *PLoS one* **4**, e6843 (2009).
47. Bligh, E. G. & Dyer, W. J. A rapid method of total lipid extraction and purification. *Can. J. Biochem. Physiol.* **37**, 911–917 (1959).
48. Sekiya, M. *et al.* Polyunsaturated fatty acids ameliorate hepatic steatosis in obese mice by SREBP-1 suppression. *Hepatology* **38**, 1529–1539 (2003).
49. Kumadaki, S. *et al.* Inhibition of ubiquitin ligase F-box and WD repeat domain-containing 7alpha (Fbw7alpha) causes hepatosteatosis through Kruppel-like factor 5 (KLF5)/peroxisome proliferator-activated receptor gamma2 (PPARgamma2) pathway but not SREBP-1c protein in mice. *J. Biol. Chem.* **286**, 40835–40846 (2011).

Acknowledgements

The authors thank Katsuko Okubo, Yuko Tamai and Chizuko Fukui for technical assistance. The authors also thank Dr. Tappei Takada (University of Tokyo) for discussion and helpful suggestions. This work was supported by Grants-in-Aid for Scientific Research 21390275 (to H. S.), 22117502 (to H. S.), 21689025 (to T. M.) and Program to Disseminate Tenure Tracking System (to T. M.) from the Ministry of Science, Education, Culture, and Technology of Japan, the Kowa Life Science Foundation (to T. M.) and the Suzuken Memorial Foundation International (to T. M.).

Author Contributions

M.K., T.M. and H.S. designed the project; M.K., T.M., R.M., R.S., N.K., H.T., N.O., T.K. and H.O. performed experiments; K.I. and Y.A. contributed analysis tools; M.K., T.M., S.H., Y.T., K.K., H.I., S.Y., H.S., N.Y., T.F., Y.N., N.Y. and H.S. analysed and interpreted data; and M.K., T.M. and H.S. prepared the manuscript. All authors reviewed the manuscript.

Additional Information

Supplementary information accompanies this paper at <http://www.nature.com/srep>

Competing financial interests: The authors declare no competing financial interests.

How to cite this article: Kuba, M. *et al.* Absence of *Elovl6* attenuates steatohepatitis but promotes gallstone formation in a lithogenic diet-fed *Ldlr*^{-/-} mouse model. *Sci. Rep.* **5**, 17604; doi: 10.1038/srep17604 (2015).



This work is licensed under a Creative Commons Attribution 4.0 International License. The images or other third party material in this article are included in the article's Creative Commons license, unless indicated otherwise in the credit line; if the material is not included under the Creative Commons license, users will need to obtain permission from the license holder to reproduce the material. To view a copy of this license, visit <http://creativecommons.org/licenses/by/4.0/>

Supplementary Information

Absence of *Elovl6* attenuates steatohepatitis but promotes gallstone formation in a lithogenic diet-fed *Ldlr*^{-/-} mouse model

Motoko Kuba, Takashi Matsuzaka, Rie Matsumori, Ryo Saito, Naoko Kaga, Hikari Taka,

Kei Ikehata, Naduki Okada, Takuya Kikuchi, Hiroshi Ohno, Song-iee Han, Yoshinori

Takeuchi, Kazuto Kobayashi, Hitoshi Iwasaki, Shigeru Yatoh, Hiroaki Suzuki, Hirohito

Sone, Naoya Yahagi, Yoji Arakawa, Tsutomu Fujimura, Yoshimi Nakagawa,

Nobuhiro Yamada, and Hitoshi Shimano

Supplementary Table S1

The Composition of the Lithogenic Diet (LD)

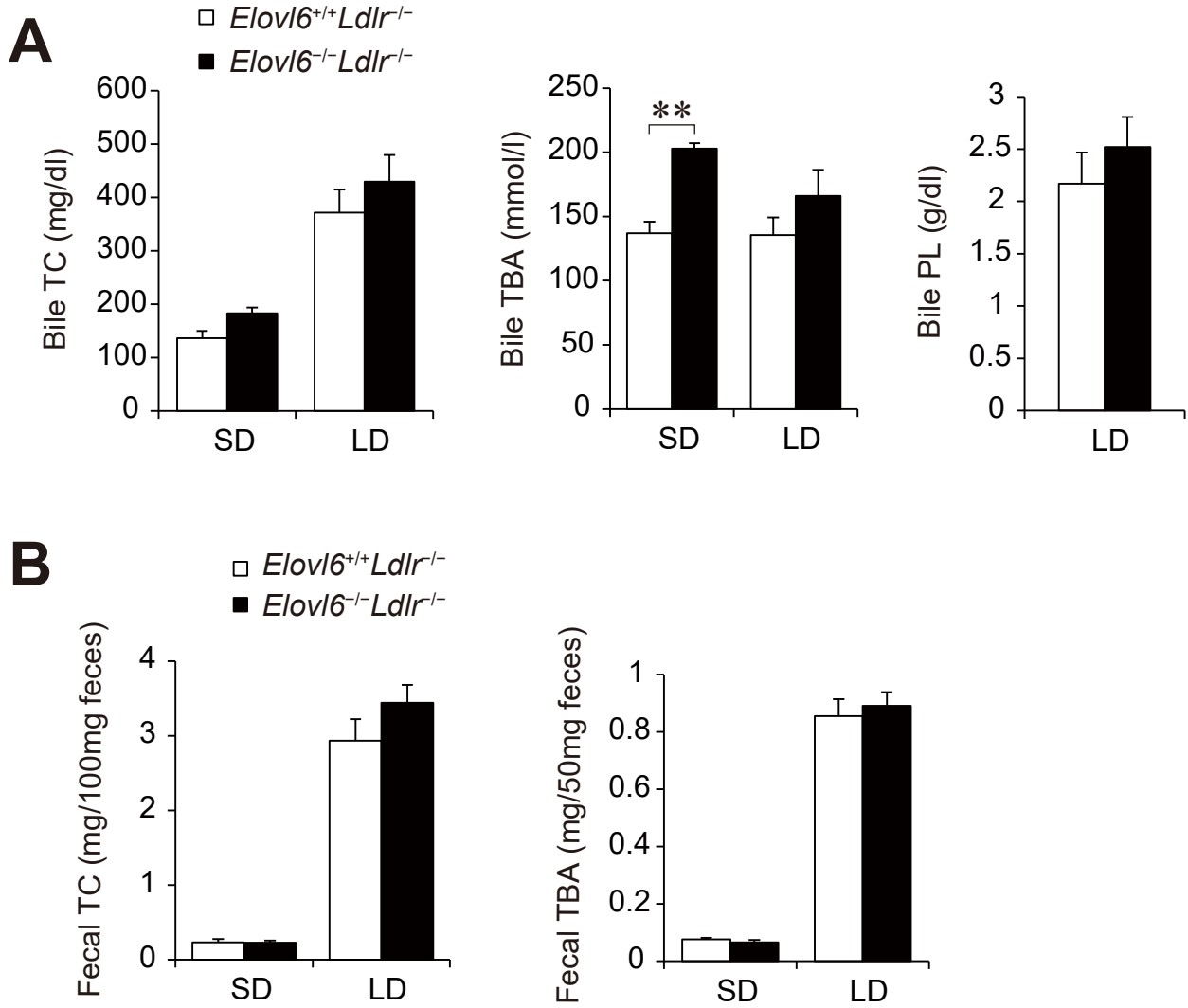
Composition	%
Cacao butter	7.500
Cholesterol	1.250
Cholate	0.500
Milk casein	7.500
Cellulose	1.250
Vitamin mix	1.000
Mineral mix	1.000
Sucrose	1.625
Glucose	1.625
Dextran	1.625
Choline chloride	0.125
Lard	3.000
CRF-1	72.000
Total	100.000

Supplementary Table S2

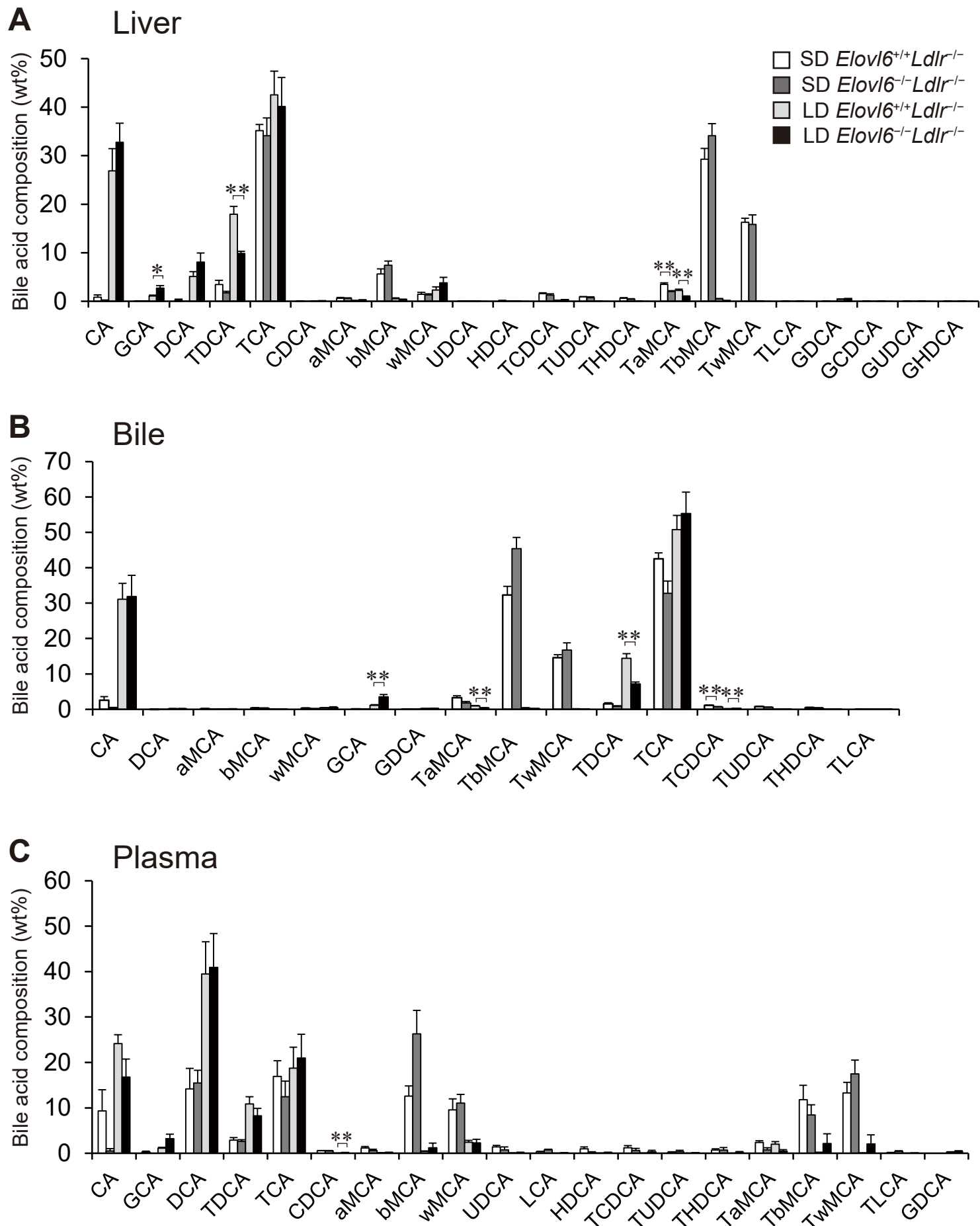
Sequence information for the quantitative Real-time PCR analysis

Gene name	Forward primer (5' to 3')	Reverse primer (5' to 3')
<i>Acat2</i>	CCCGTGGTCATCGTCTCAG	GGACAGGGCACCATTGAAGG
<i>Nr1h3</i>	AGCAACAGTGTAACAGGCGCT	ACGATGGCCAGCTCAGTAAAGT
<i>Ces3a</i>	ACTGGGACCTCTTCGGTTCT	GGTGAATCTGCTGTTGCTCA
<i>Ces3b</i>	CACAGACCGCATGGTAAATG	TTGATGCTGGCATCTCTCAC
<i>Nr1h4</i>	CTCTGCTCACAGCGATCGTC	CACCGCCTCTCTGTCTTGA
<i>Nr5a2</i>	ATACAAACTCCCGCTGATCG	AAGTCGCGTTCAACAACCTC
<i>Nr0b2</i>	CGATCCTCTTCAACCCAGATG	AGGGCTCCAAGACTTCACACA
<i>Cyp7a1</i>	GCTGAGAGCTTGAAGCACAGA	TTGAGATGCCAGAGGATCAC
<i>Cyp8b1</i>	CTAGGGCCTAAAGGTTTCGAGT	GTAGCCGAATAAGCTCAGGAAG
<i>Cyp27a1</i>	CCAGGCACAGGAGAGTACG	GGGCAAGTGCAGCACATAG
<i>Cyp7b1</i>	AGCCGATTATCAGCGAAAGCC	GCATCCAAAGGTTTGCCTTGT
<i>Slc10a1</i>	AGGGGGACATGAACCTCAG	TCCGTCGTAGATTCCTTTGC
<i>Slco1a1</i>	ACTCCATAATGCCCTTGG	TAATCGGGCCAACAATCTTC
<i>Abcb11</i>	CAATGTTTCAGTTCCTCCGTTCA	TCTCTTTGGTGTTGTCCCATA
<i>Abcc1</i>	GATGGCTCCGATCCACTCT	AGGTAGAAACAAGGCACCCA
<i>Abcc2</i>	TCCAGGACCAAGAGTTTGC	TCTGTGAGTGCAAGAGACAGGT
<i>Abcc3</i>	TGAAGACTGCACCGTACTGAC	AGAAACCCTTGGAATGCATC
<i>Abcc4</i>	AGCTTCAACGGTACTGGGATA	TCGTCGGGGTCATACTTCTC
<i>Slc51b</i>	AGAGAAAGCTGCAGCCAATG	CCAGGACCAGGATGGAATAA
<i>Cd14</i>	GAAGCAGATCTGGGGCAGTT	CGCAGGGCTCCGAATAGAAT
<i>Cybb</i>	TTGGGTCAGCACTGGCTCTG	TGGCGGTGTGCAGTGCTATC

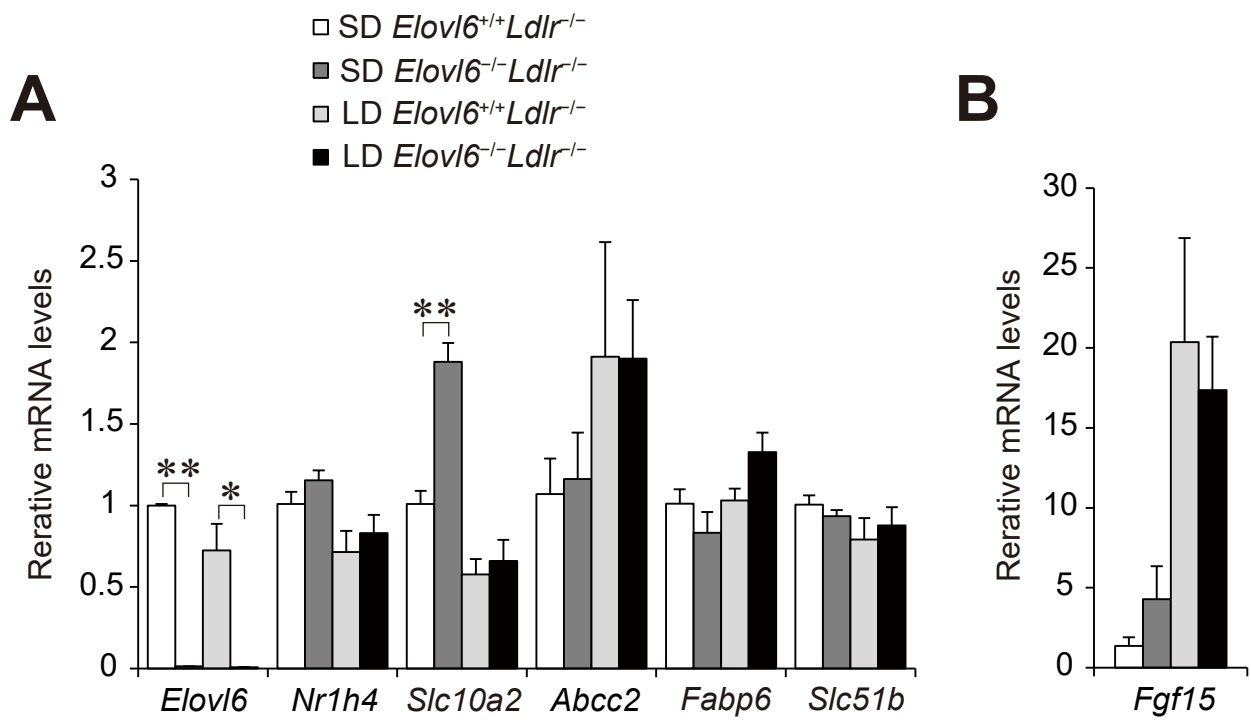
Supplementary Figure S1



Supplementary Figure S2



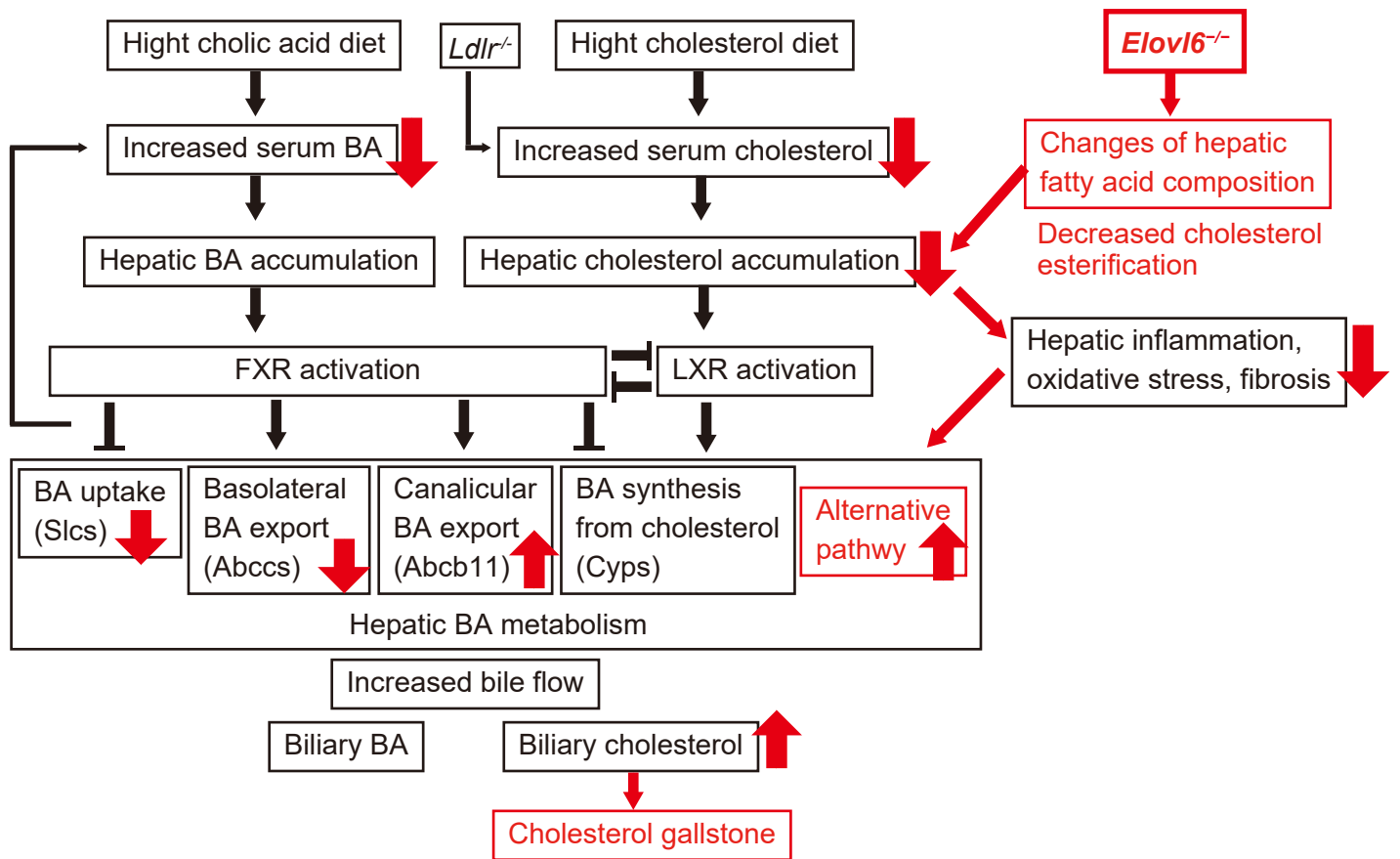
Supplementary Figure S3



Supplementary Figure S4

Effects of LD on $Ldlr^{-/-}$

Effects of LD on $Elovl6^{-/-}$



Supplementary Figure Legends

Supplementary Figure S1. Bile and fecal lipid profiles of LD-fed *Ldlr*^{-/-} mice lacking Elov16.

(A) Bile total cholesterol (TC), total bile acid (TBA), and phospholipid (PL) levels (n = 3–8 per group) and (B) fecal TC and TBA levels (n = 7–10 per group) of *Elov16*^{+/+}*Ldlr*^{-/-} and *Elov16*^{-/-}*Ldlr*^{-/-} mice fed a SD or a LD for 4 weeks.

Supplementary Figure S2. Bile acid composition in (A) liver, (B) bile, and (C) plasma in

Elov16^{+/+}*Ldlr*^{-/-} and *Elov16*^{-/-}*Ldlr*^{-/-} mice fed a SD or a LD for 4 weeks (n = 3–9 per group).

individual BA species were examined by LC/MS. CA, cholic acid; GCA, glycocholic acid; DCA, deoxycholic acid; TDCA, taurodeoxycholic acid; TCA, taurocholic acid; CDCA, chenodeoxycholic acid; α MCA, alpha-muricholic acid; β MCA, beta-muricholic acid; ω MCA, omega-muricholic acid; UDCA, ursodeoxycholic acid; HDCA, hyodeoxycholic acid; TCDCA, taurochenodeoxycholic acid; TUDCA, tauroursodeoxycholic acid; THDCA, taurouhyodeoxycholic acid; T α MCA, tauro- α -muricollic acid; T β MCA, tauro- β -muricollic acid; T ω MCA, tauro- ω -muricollic acid; LCA, lithocholic acid; TLCA, tauroolithocholic acid; GDCA, glycodeoxycholic acid; GCDCA, glycochenodeoxycholic acid; GUDCA, glycoursodeoxycholic acid; GHDCa, glycouhyodeoxycholic acid. * $P < 0.05$, ** $P < 0.01$.

Supplementary Figure S3. Quantitative real-time PCR (qPCR) analysis of genes involved in bile acid homeostasis in the ileum. *Elov16^{+/+}Ldlr^{-/-}* and *Elov16^{-/-}Ldlr^{-/-}* mice were fed a SD or a LD for 4 weeks and sacrificed following 4 h of food deprivation (n = 4–7 per group). qPCR analysis of genes for (A) *Elov16*, *Nr1h4*, *Slc10a2*, *Abcc2*, *Fabp6*, *Slc51b* and (B) *Fgf15*. * $P < 0.05$, ** $P < 0.01$.

Supplementary Figure S4. Proposed mechanism of *Elov16*-mediated metabolic alteration in LD-induced liver injury and gallstone formation.

Supplementary Methods

Individual bile acid analysis by Liquid Chromatography/Mass Spectrometry

We determined individual bile salt compositions by liquid chromatography/mass spectrometry.

BA standards were purchased from Sigma. For liver samples, approximately 100 mg of liver was homogenized in 2.5 volumes of H₂O. d₄-CA (Internal standard: IS) and 400 µl of ice-cold ethanol were added to 200 µl liver homogenate. Samples were vortexed, centrifuged, and the supernatants were evaporated before being reconstituted in a 200 µl of 50:50 solution of ethanol and water. For plasma samples, 450 µl of ice-cold EtOH was added to 50 µl plasma-spiked with IS, vortexed, and centrifuged. The supernatants were evaporated and reconstituted in a 100 µl of 50:50 solution of ethanol and water. Bile samples were diluted 100- and 2000-fold with a 50:50 solution of ethanol and water, and IS was added. The LC system used was a HPLC (Gilson) equipped with an autoinjector. The HPLC was connected to a TSQ Quantum Ultra (Thermo Scientific). Individual BAs were eluted with gradient at a 0.2 ml/min flow rate for a mobile phase A (10 mM AcONH₄ in H₂O) and mobile phase B (10 mM AcONH₄ in a 23:17 solution of CH₃CN and ethanol). The samples were eluted with 80% mobile phase A and 20% mobile phase B for an initial 5 min after injection, and then with a linear gradient of mobile phase B of 20% to 75% over 55 min, which was held for 5 min. The injection volume of all samples was 5 µl. Quantitative analysis was performed in negative ionization mode using the selected reaction

monitoring transitions specific for each BA.